Electronic Supplementary Information

# Two-photon Fluorescence Imaging and Ratiometric Quantification of Mitochondrial Monoamine Oxidase-A in Neurons

Yuxiao Mei, Zhichao Liu, Meijun Liu, Jiacheng Gong, Xiao He, Qi-Wei Zhang*, and Yang Tian*

*School of Chemistry and Molecular Engineering, East China Normal University, Dongchuan Road 500, Shanghai 200241, P.R. China*

*E-mail: qwzhang@chem.ecnu.edu.cn; ytian@chem.ecnu.edu.cn*

**Contents**

# 1. Experimental Section

## Reagents and Chemicals

All chemicals were purchased from commercial suppliers and without further purification and modification. 4-Bromo-1,8-naphthalic anhydride, adenosine monophosphate (AMP), methanol (MeOH), ethanol (EtOH), Dichloromethane, 1,4-Dioxane, Acetonitrile, ,3-dibromopropane, potassium phthalimide and hydrazine monohydrate were purchased from Adamas Reagent Co., Ltd. (Shanghai, China). NaCl, KCl, $NaH_2PO_4$, $Na_2HPO_4$, $KH_2PO_4$, $Na_2SO_3$, $Na_2SO_4$, $CaCl_2$, $FeCl_3$, $FeCl_2$, $CuCl_2$, CuCl, $MgCl_2·6H_2O$, $NiCl_2·6H_2O$, $Zn(NO_3)_2·6H_2O$, $CoCl_2·6H_2O$, $H_2O_2$ were purchased from Sinopharm Chemical Reagent Co., Ltd. (Shanghai, China). Glutathione (GSH), L-cysteine (Cys), L-arginine (Arg), L-glutamine (Glu), L-histidine (His), glycine (Gly), L-isoleucine (Iso), Lysine (Lys), L-leucine (Leu), L-phenylalanine (Phe), L-methionine (Met), L-serine (Ser), L-valine (Val), L-threonine (Thr), bovine serum albumin (BSA), acetyl cholinesterase (AchE), butyrylcholinesterase (BuChE) were purchased from Aladdin Chemistry Co. Ltd. (China). Dopamine (DA), ascorbic Acid (AA), 5-hydroxytryptamine (5-HT), glucose, uric acid (UA), Norepinephrine (NE). Superoxide anion ($O_2^{\bullet-}$) was prepared from a classical XA/XOD system. Its concentration was determined by measuring the reduction of ferricytochrome c ($\varepsilon_{550}$=21.1$mM^{-1}cm^{-1}$) spectrophotometrically using an UV vis spectrophotometer. Ferricytochrome c reacts with the generated $O_2^{\bullet-}$ by the univalent pathway as follows: cytochrome $C^{3+}$ + $O_2^{\bullet-}$ = cytochrome $C^{2+}$ + $O_2$, which shows a 1:1 reaction relationship [S1, S2]. Hydroxyl radical (•OH) was derived from Fenton reaction ($Fe_2$+/$H_2O_2$ = 1:5). Nitric oxide (NO) was generated from Sodium nitroprusside dihydrate. Peroxynitrite ($ONOO^-$) was generated by the reaction of $NaNO_2$ with $H_2O_2$. $SO_2$ and $H_2S$ were derived from $Na_2SO_3$ and $Na_2S$, respectively. Alkyl peroxyl radical (ROO•) was obtained by heating α, α′-azodiisobutyramidine dihydrochloride (AAPH) in water at 37 °C.

Singlet oxygen ($^1O_2$) was produced by the reaction between $H_2O_2$ and NaClO. HClO was originated from NaClO. Angeli's salt (AS) was used as HNO donor. The concentration of $O_2^{\bullet-}$, $ONOO^-$, $H_2O_2$, and HClO were obtained by the UV–vis absorption spectrophotometry.

**Instruments**

The $^1H$ NMR and $^{13}C$ NMR spectra were obtained from a 500 MHz Bruker NMR spectrometer (Bruker, Germany). The mass spectra were detected by a Bruker ESI time-of-flight MS system (Bruker, Germany). The fluorescence spectrum and the UV-vis absorption spectrum was recorded by using a Hitachi F-4500 fluorescence spectrometer (Hitachi, Japan) and a Hitachi UH-5300 spectrometer (Hitachi, Japan), respectively. The fluorescence imaging was obtained from a Leica TCS SP8 confocal laser scanning microscope (Leica, Germany) equipped with two-photon laser (Chameleon Ultra II, Coherent, UK). The fluorescence lifetime decay curves and imaging were measured by a time-correlated single photon counting (TCSPC) module SyPhotime-64 (Becker & Hickl, Germany). The cytotoxicity assays were measured by Varioskan LUX multimode microplate reader (Thermo Fisher scientific, USA). The apoptosis assay was carried out by a FACS Calibur flow cytometry (Becton, Dickinson and Company, USA). The fresh mouse brain tissue slices were obtained using a Leica VT3000 vibrating-blade microtome (Germany) with a thickness of about 300 μm.

**Cell culture**

All animal experiments were performed according to the guidelines of the Care and Use of Laboratory Animals formulated by the Ministry of Science and Technology of China and were approved by the Animal Care and Use Committee of East China Normal University (approval no. m+ R20190304, Shanghai, China). The acquisition and cultivation of neurons were conducted

as a previous reported procedure. Newborn within 24 hours C57BL/6 wild-type mice were anesthetized by halothane, and then their brains were removed quickly and put in Hanks' balanced salt solution (HBSS, free $Mg^{2+}$ and $Ca^{2+}$) at 0 °C. Tissues of the cortex were stripped out and then incubated with papain at 37 °C for 12 min, after that the they were dispersed into poly-d-lysine-coated 35 mm Petri dishes at a density of 1 ×106 cells/dish. The neurons were cultured with neurobasal medium containing L-Glutamine and B27 and the medium was changed three times a week. After maintained at 37 °C in a humidified atmosphere with 5% $CO_2$ incubator for a week, the neurons could be used for imaging.

**Cytotoxicity and apoptosis assay**

The cytotoxicity assays were measured by 3-(4,5-dimethylthiazol-2-yl)-2,5-diphenyltetrazolium bromide (MTT). Neurons in 96-well plates were incubated with different concentrations of the **TMF2P** probe (0, 10, 15, 20, 25, and 30 μM) and cultured for 12 and 24 h. Then, the neurons in each well were treated with 20 μL, 5 mg/mL MTT solution and further continuously incubated for 4 h at 37 °C. After that, MTT solution was removed and 100 μL Formazan Solvent was added to each well until the crystalline formazan products were dissolved. Absorbance was next measured at 490 nm in a Varioskan LUX multimode microplate reader (Thermo Fisher scientific, USA). Cell viability was defined as the ratio of absorbance in the experimental groups to that in the blank control groups. For apoptosis assays, the Annexin V-FITC Apoptosis Detection Kit was used to determine the degree of cell apoptosis. Neurons were incubated with the **TMF2P** probe (0, 10, 30, and 50 μM) for 24 h, then they were collected with the help of EDTA-free trypsin and washed by 5 mL PBS for three times. Moreover, PBS was removed by centrifugation of 1000 rpm for 5 min and neurons were incubated with 195 μL binding buffer of Annexin V-FITC, 5 μL Annexin V-FITC and 10 μL Propidium Iodide (PI) at room temperature in the dark for 30 min. After these procedures, neurons were used for the flow cytometry and detected

at an excitation wavelength of 488 nm.

**Statistical Analysis.**

Data are expressed as means ± SD of 10 samples in each experimental group. The student t test was used to assess the statistical significance between a pair of experimental groups. P-values were generated by two-tailed t test assuming equal variance using IBM SPSS Statistics Software. The value 0.05 (*), 0.01 (**), and 0.001 (***) was assumed as the level of significance for the statistic tests (n = 20; *, P < 0.05; **, P < 0.01; ***, P < 0.001; and NS means no statistical significance per unpaired t-test).

## 2. Synthesis and characterization of TMF2P

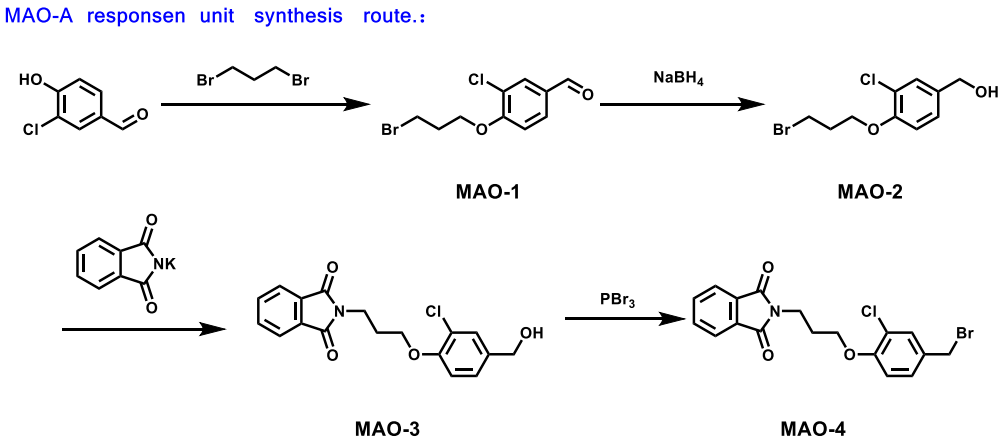


**Scheme S1**. The synthesis procedures of **MAO-4**.

**Synthesis of Compound MAO-1:** A mixture of 3-chloro-4-hydroxybenzaldehyde (1.56 g, 10 mmol), $K_2CO_3$ (2.76 g, 20 mmol), 1,3-dibromopropane (2 mL, 20 mmol) were dissolved in acetonitrile (30 mL) and methanol (5 mL), the reaction mixture was stirred and refluxed for 8 h. After the mixture was cooled to room temperature, the filter residue was removed by filtration and the resulting organic phase was finally dried under vacuum by evaporation to remove the solvent. The residue was purified by column

chromatography (PE: EA = 40: 1, v/v) to obtain **MAO-1**. $^{1}$H NMR (500 MHz, 298 K, DMSO-$d_6$): δ 9.88 (s, 1H), 7.97-7.91 (m, 1H), 7.41-7.39 (d, $J$ = 10.0 Hz, 1H), 4.31 (t, $J$ = 10.0 Hz, 2H), 3.70 (m, 2H), 2.34-2.32 (m, 2H). $^{13}$C-NMR (125 MHz, 298 K, $CDCl_3$ $d$): δ 189.6, 158.9, 131.2, 130.5, 130.4, 124.0, 112.6, 66.6, 31.9, 29.5. HR-ESI-MS m/z: $[M+Na]^+$ calcd for $[C_{10}H_{10}BrClNO_2Na]^+$, 298.9450; found, 298.9449.

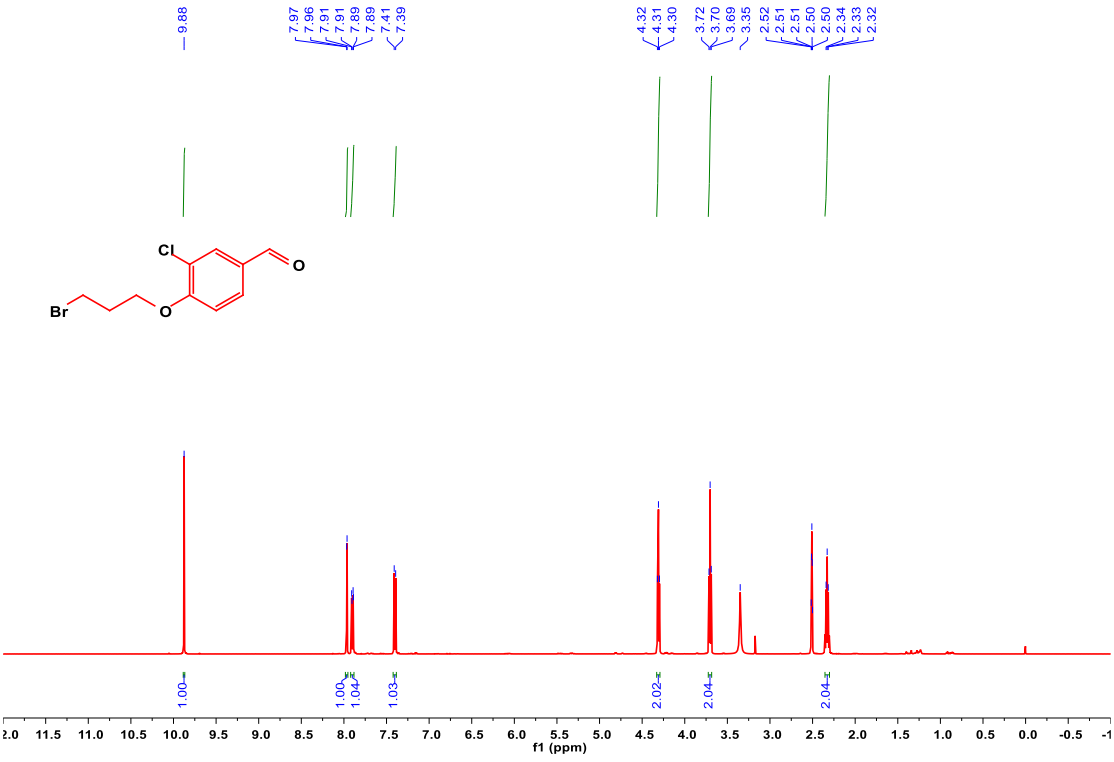


**Fig. S1**. $^{1}$H NMR spectrum of Compound **MAO-1**.

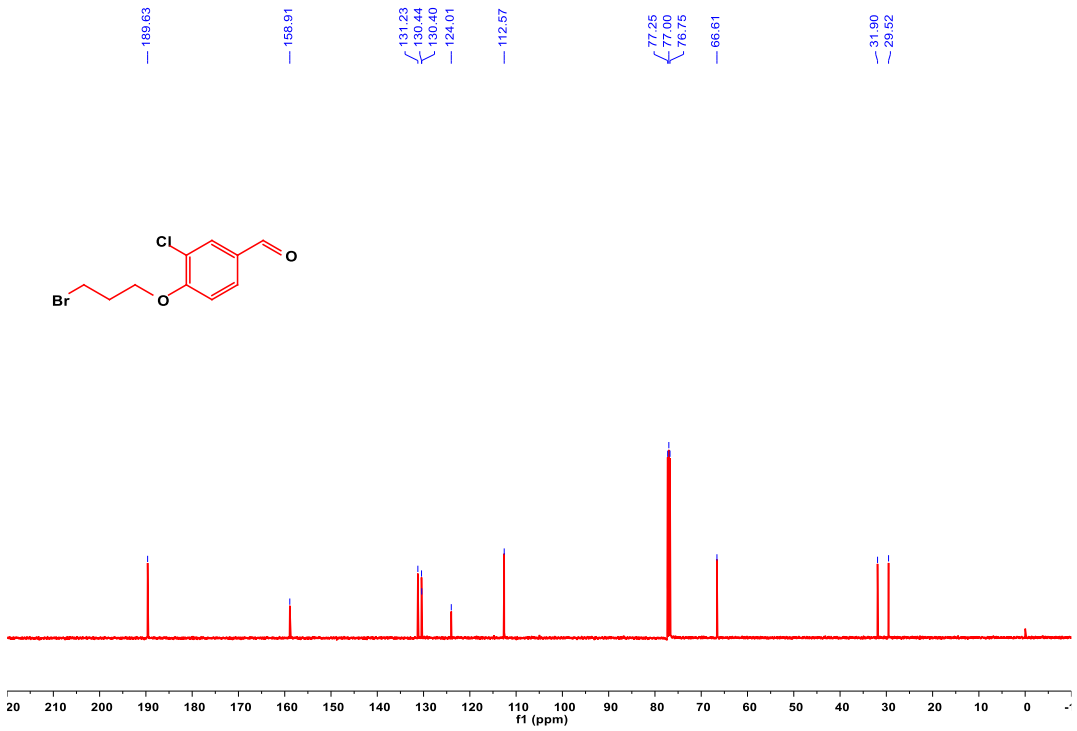


**Fig. S2**. $^{13}C$ NMR spectrum of Compound **MAO-1**.

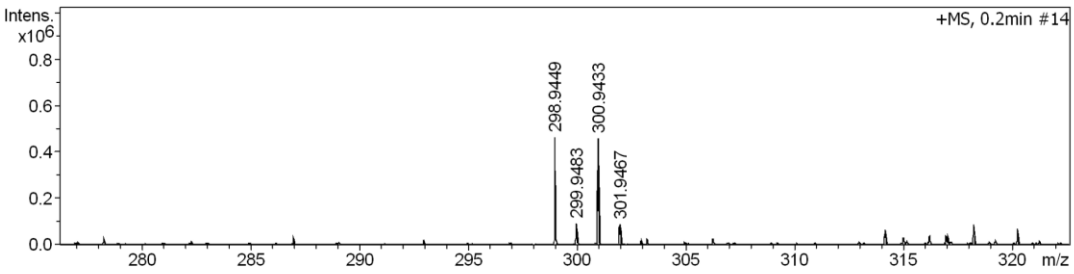


**Fig. S3**. HR-MS spectrum of Compound **MAO-1**.

**Synthesis of Compound MAO-2:** $NaBH_4$ (1.3 g, 10 mmol) was added slowly into a suspension of MAO-1 (1.38 g, 5 mmol) in $CH_3OH$ (30 mL) at 0 °C. After 30 min, the resulting suspension was stirred at room temperature for 2 h. Then, the mixture was diluted with dichloromethane (20 mL) and washed three times with water (20 mL). The organic layer was separated and dried over anhydrous $Na_2SO_4$. The solvent was removed by evaporation under reduced pressure, The residue was purified by column chromatography (PE: EA = 20:1 to 5:1, v/v) to obtain **MAO-2**. $^1$H NMR (500 MHz, 298 K, $CDCl_3$-*d*): δ 7.39 (s, 1H), 7.23-7.21 (t, *J* = 10.0 Hz, 1H), 6.93-6.91 (d, *J* = 10.0 Hz, 1H), 5.01 (s, 2H), 4.18-4.16 (t, *J* = 10.0 Hz, 2H), 3.67-3.65 (t, *J* = 10.0 Hz, 2H), 2.38-2.35 (t, *J* = 15.0 Hz, 2H). $^{13}$C NMR (125 MHz, 298 K, $CDCl_3$-*d*): δ 153.6, 134.4, 129.2, 126.4, 123.1, 113.6, 66.6, 64.3, 32.2, 29.9. HR-ESI-MS m/z: $[M+Na]^+$ calcd for $[C_{10}H_{12}BrClNO_2Na]^+$, 300.9607; found, 300.9603.

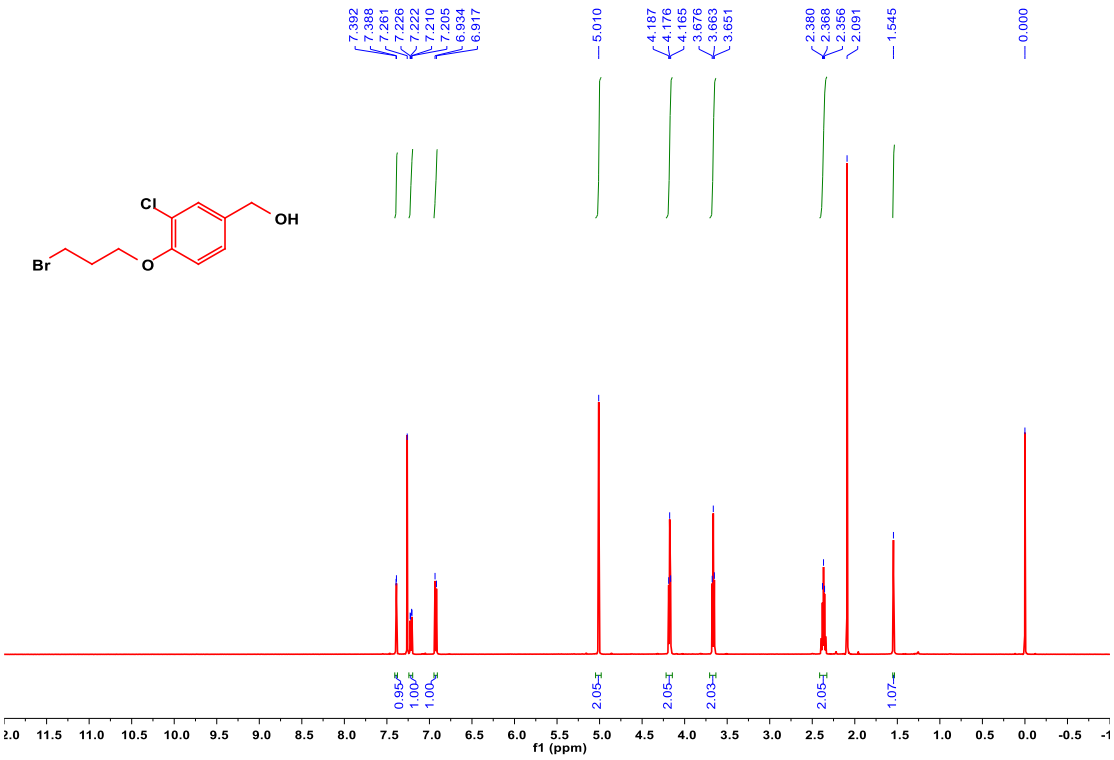


**Fig. S4**. $^1$H NMR spectrum of Compound **MAO-2**.

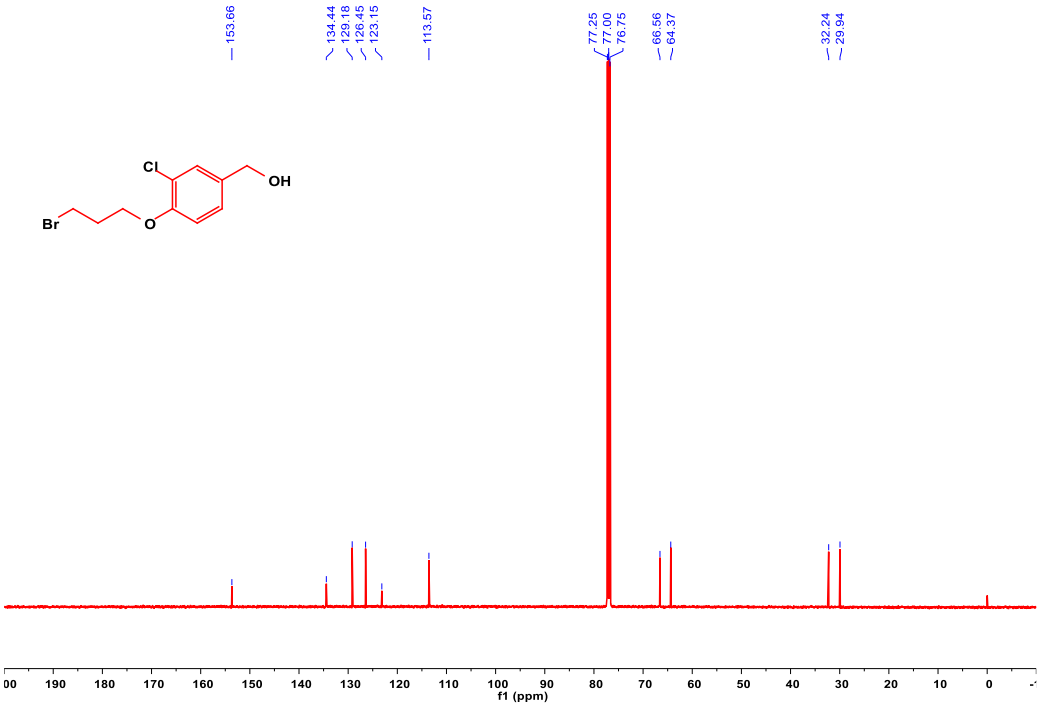


**Fig. S5**. $^{13}C$ NMR spectrum of Compound **MAO-2**.

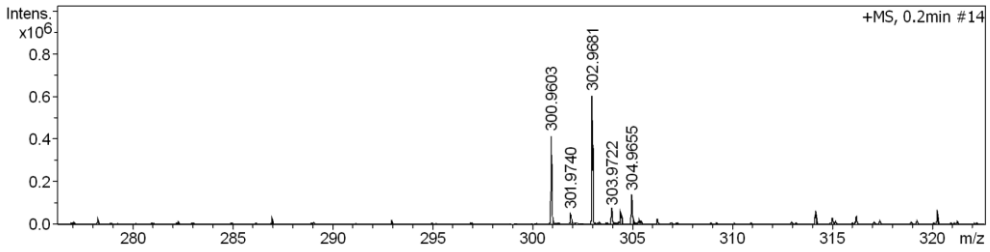


**Fig. S6**. HR-MS spectrum of Compound **MAO-2**.

**Synthesis of Compound MAO-3:** A mixture of MAO-2 (560 mg, 2 mmol) and potassium phthalimide (720 mg, 4 mmol) in anhydrous 10 ml DMF was heat at 100 °C and stir for 12 h under $N_2$ atmosphere. Cool the mixture to room temperature and remove the solvent by reduced pressure distillation. Then the crude product was purified by column chromatography (PE: EA =50:1 to 10:1, v/v) to obtain **MAO-3**. $^1H$ NMR (500 MHz, 298 K, DMSO-$d_6$): δ 7.85-7.80 (t, $J$ =

10.0 Hz, 4H), 7.28 (d, $J$ = 2.0 Hz, 1H), 7.19 (dd, $J_1$ = 2.5 Hz, $J_2$ = 8.5 Hz, 1H), 7.03-7.02 (d, $J$ = 8.5 Hz, 1H), 5.18-5.16 (t, $J$ = 11.5 Hz, 2H), 4.40-4.39 (m, $J$ = 5.5 Hz, 2H), 4.10-4.07 (t, $J$ = 5.5 Hz, 2H), 3.81-3.78 (t, $J$ = 13.5 Hz, 2H), 2.17-2.14 (t, $J$ = 5.5 Hz, 2H).$^{13}$C NMR (125 MHz, 298 K, DMSO-$d_6$): δ 168.4, 152.9, 136.3, 134.6, 132.3, 128.4, 126.7, 123.3, 121.4, 113.8, 67.2, 62.3, 35.6, 28.1. HR-ESI-MS m/z: $[M+Na]^+$ calcd for $[C_{18}H_{16}ClNO_2Na]^+$, 378.0650; found, 378.0653.

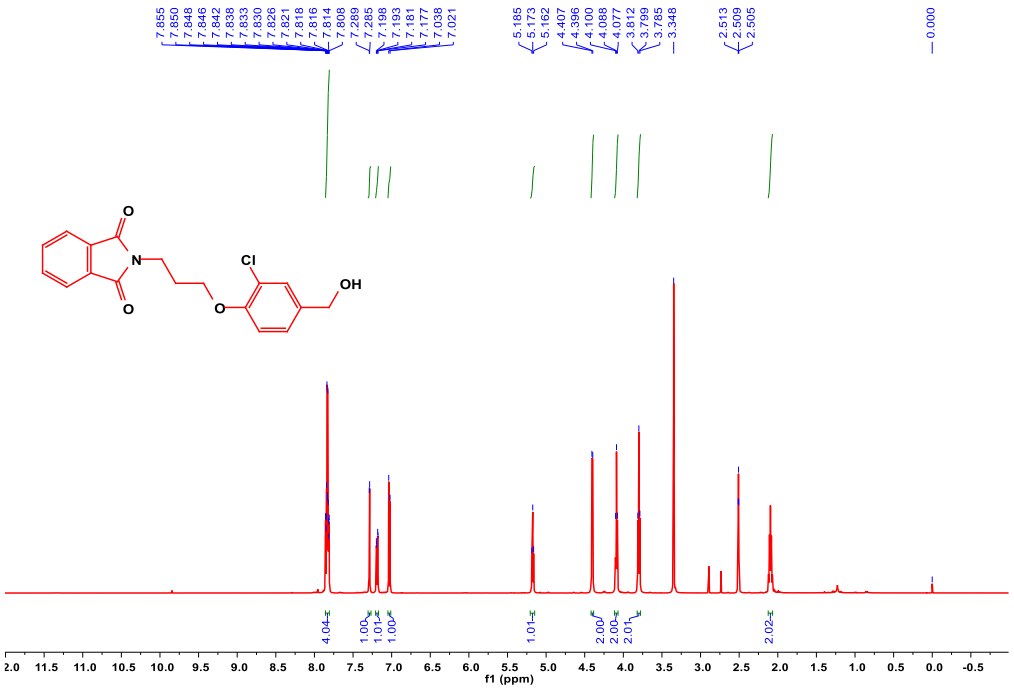


**Fig. S7**. $^1$H NMR spectrum of Compound **MAO-3**.

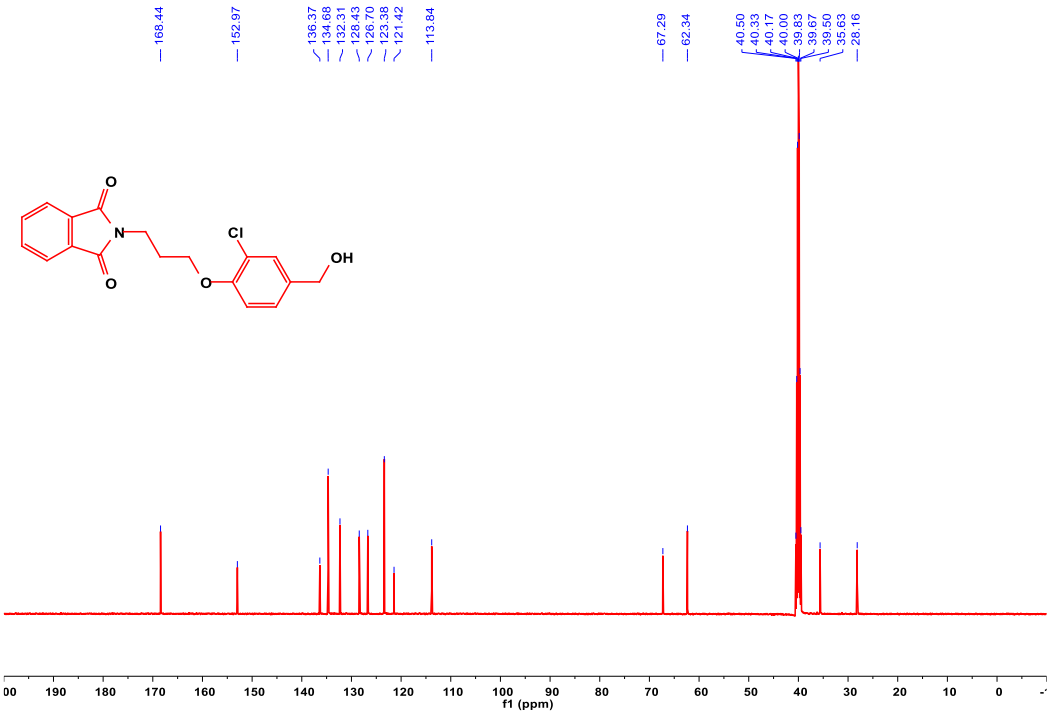


**Fig. S8**. $^{13}C$ NMR spectrum of Compound **MAO-3**.

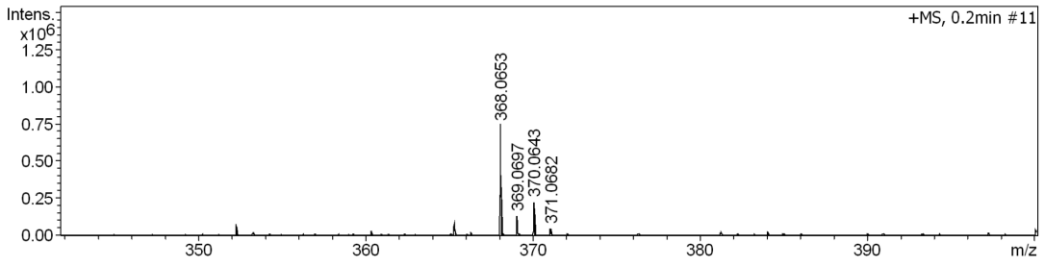


**Fig. S9**. HR-MS spectrum of Compound **MAO-3**.

**Synthesis of Compound MAO-4:** Tri-bromophosphine (0.19 mL, 2.0 mmol) was added dropwise into a solution of compound MAO-3 (345 mg, 1.0 mmol) in dichloromethane (30 mL) at 0 $^0C$. The resulting reaction mixture was warmed up to room temperature and stirred for 2 h. Then, the mixture was diluted with dichloromethane (20 mL) and washed three times with water (20 mL). The organic layer was separated and dried over anhydrous $Na_2SO_4$. The solvent was removed by evaporation under reduced pressure, Then the crude product was purified by column chromatography (PE: EA =50:1 to 10:1, v/v) to obtain

**MAO-4**. $^{1}$H-NMR (500 MHz, 298 K, $CDCl_3$-*d*): δ 7.84-7.82 (m, 2H), 7.71-7.70 (dd, $J_1$ = 3.5 Hz, $J_2$ = 5.5 Hz, 2H), 7.35-7,34 (d, $J$ = 2.5 Hz, 2H), 7.21-7.19 (m, 1H), 6.85-6.83 (d, $J$ = 8.5 Hz, 1H), 4.14 (s, 2H), 4.11-4.08 (t, $J$ = 7.0 Hz, 2H), 3.95-3.93 (t, $J$ = 6.5 Hz, 2H), 2.27-2.23 (dd, $J_1$ = 6.5 Hz, $J_2$ = 12.5 Hz, 2H). $^{13}$C-NMR (125 MHz, 298 K, $CDCl_3$-*d*): δ 168.3, 154.3, 133.9, 132.1, 130.9, 128.4, 123.2, 123.0, 113.1, 67.0, 35.4, 32.6, 28.3 HR-ESI-MS m/z: $[M+Na]^+$ calcd for $[C_{18}H_{15}BrClNO_3Na]^+$, 429.9820; found, 429.9818.

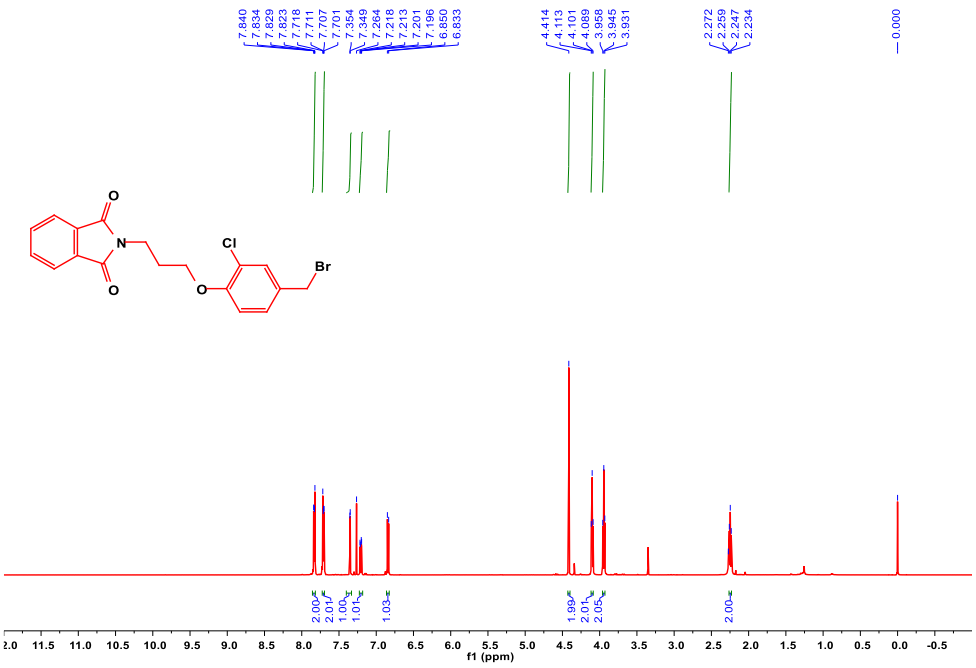


**Fig. S10**. $^{1}$H NMR spectrum of Compound **MAO-4**.

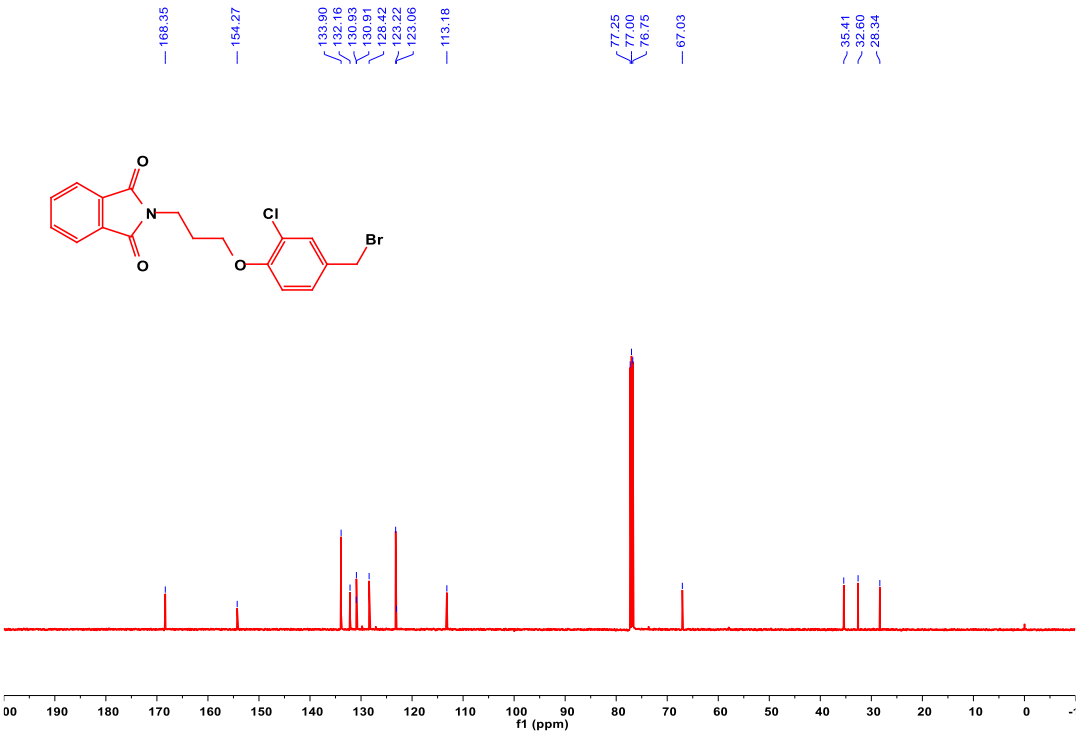


**Fig. S11**. $^{13}C$ NMR spectrum of Compound **MAO-4**.

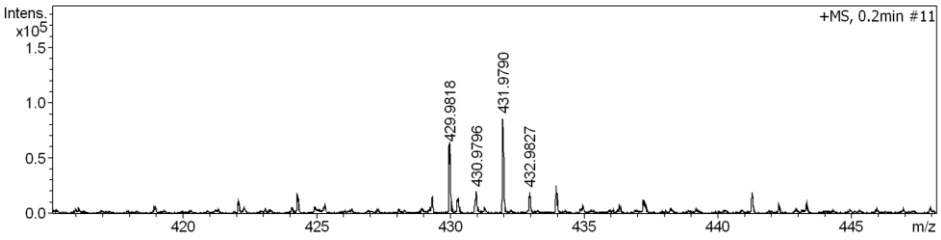


**Fig. S12**. HR-MS spectrum of Compound **MAO-4**.

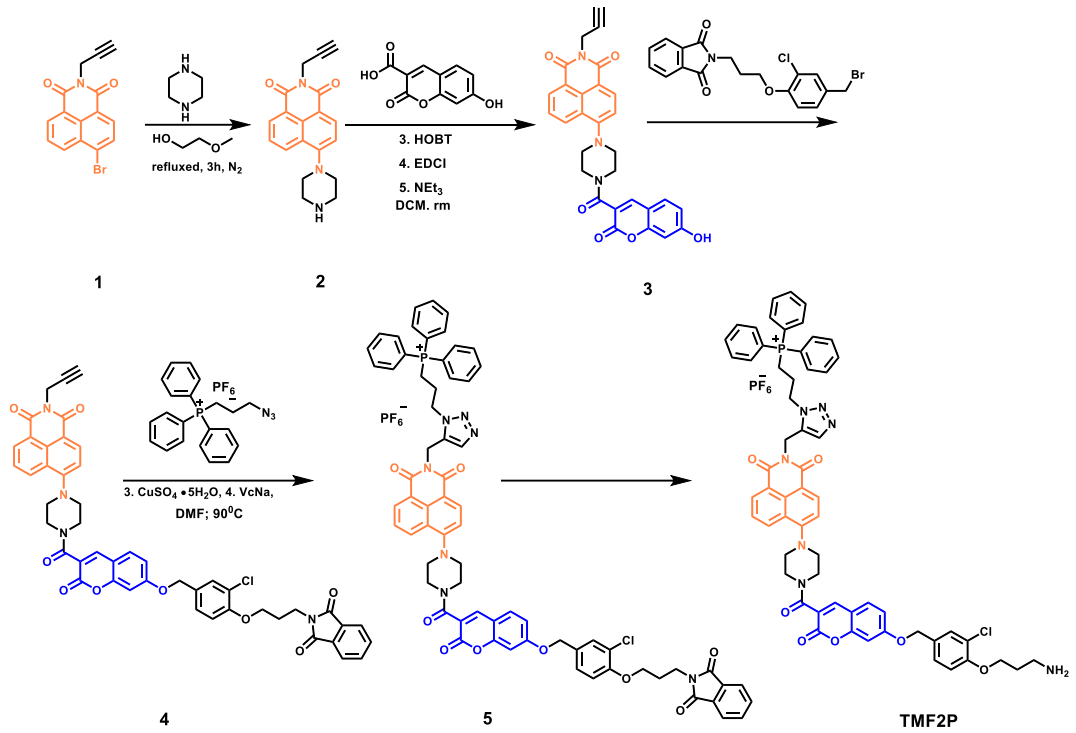


**Scheme S2**. The synthesis procedures of **TMF2P**.

**Synthesis of Compound 1:** 4-bromo-1,8-naphthalic anhydride (2.77 g, 10.0 mmol) and prop-2-yn-1-amine (1.15 g, 20.0 mmol) were dissolved in ethanol (40 mL). The reaction mixture was stirred and refluxed for 8 h under nitrogen atmosphere. After the solvent was evaporated under reduced pressure, the crude product was purified by silica gel column chromatography using PE/$CH_2Cl_2$ (10:1, v/v) as eluent to obtain **Compound 1** as yellow solid. $^1$H NMR (500 MHz, 298 K, $CDCl_3$-*d*): δ 8.69-8.68 (d, *J* = 7.0 Hz,), 8.59-8.57 (dd, $J_1$ = 1.0 Hz, $J_2$ = 8.5 Hz, 1H), 8.45-8.43 (d, *J* = 8.0 Hz, 1H), 8.05-8.03 (d, *J* = 8.0 Hz, 1H), 7.87-7.84 (dd, $J_1$ = 7.5 Hz, $J_2$ = 9.5 Hz, 1H), 4.95 (d, *J* = 2.5 Hz, 1H), 3.15-3.11 (m, 1H). $^{13}$C NMR (125 MHz, 298 K, $CDCl_3$-*d*): δ 162.8, 162.7, 133.6, 132.4, 131.5, 131.1, 128.9, 128.1, 122.7, 121.8, 78.3, 29.5. HR-ESI-MS m/z: $[M+Na]^+$ calcd for $[C_{15}H_8BrNO_2Na]^+$, 335.9682; found, 335.9631.

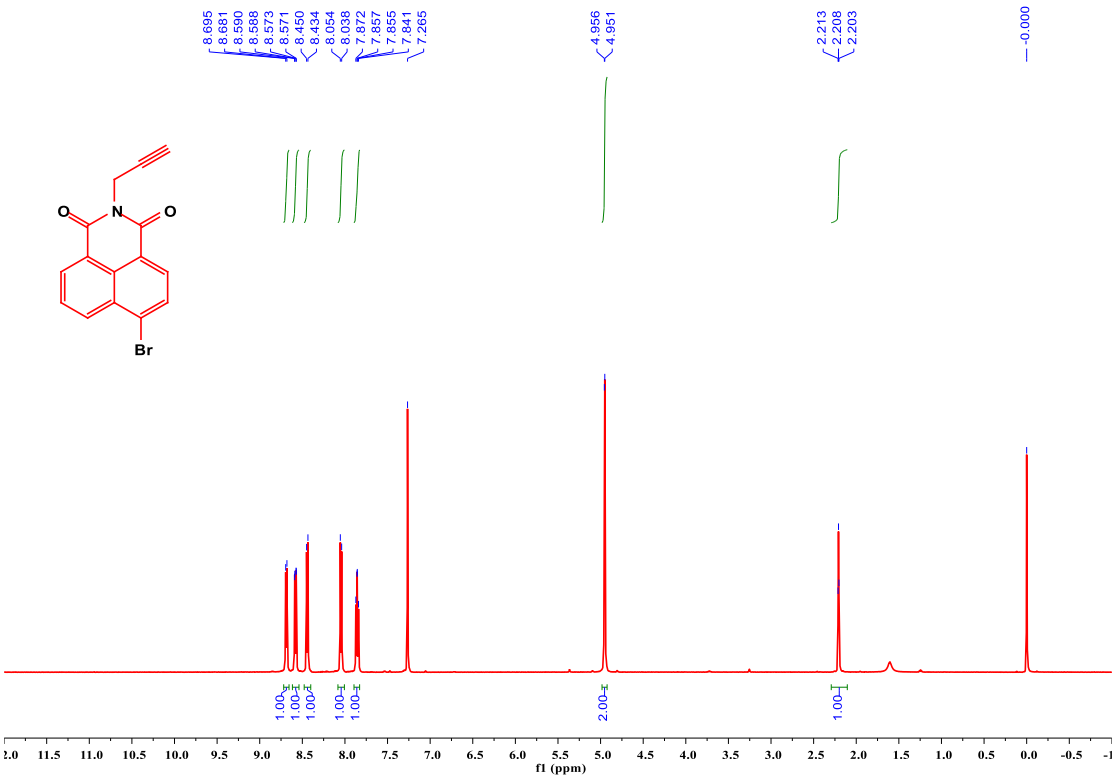


**Fig. S13**. $^{1}$H NMR spectrum of **Compound 1**.

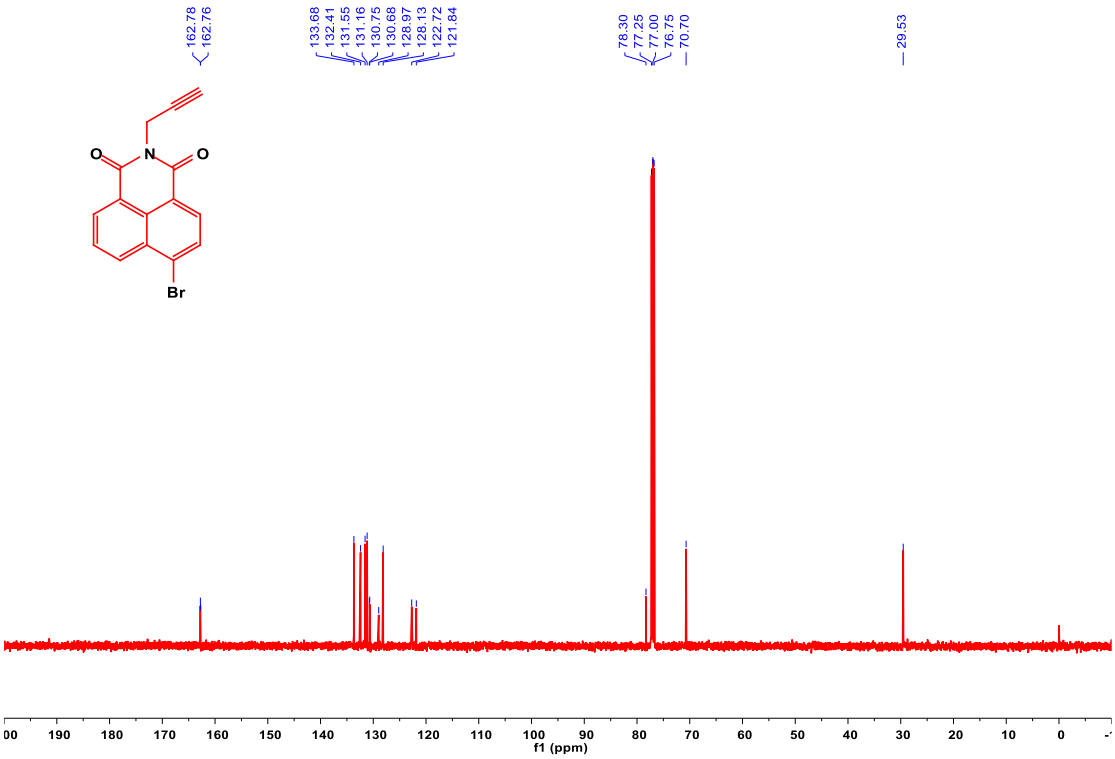


**Fig. S14**. $^{13}$C NMR spectrum of **Compound 1**.

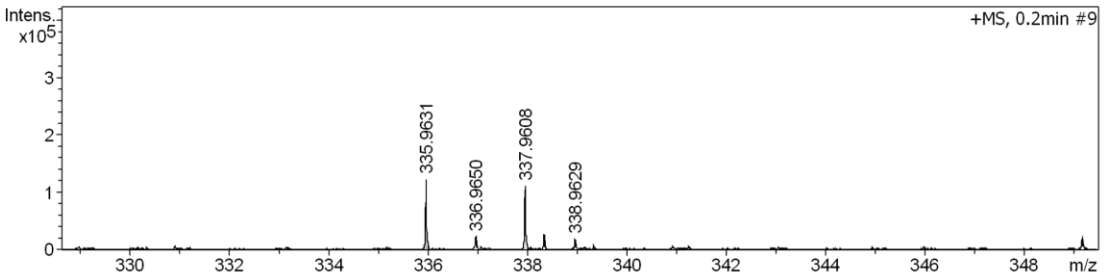


**Fig. S15**. HR-MS of **Compound 1**.

**Synthesis of Compound 2:** Piperazine (2.09 g, 24.00 mmol) and compound 1 (1.25 g, 2.40 mmol) were dissolved in methylglycol (40 mL). The reaction mixture was stirred and refluxed for 3 h under nitrogen atmosphere. After the solvent was evaporated under reduced pressure, the crude product was purified by silica gel column chromatography using $CH_2Cl_2$/MeOH (10:1, v/v) as eluent to give 1.10 g of **Compound 2** as yellow solid. $^1$H NMR (500 MHz, 298 K, DMSO-$d_6$): δ 8.45-8.35 (m, 3H), 7.78-7.75 (t, $J$ = 8.0 Hz, 1H), 7.27-7.26 (d, $J$ = 8.0 Hz, 1H), 4.74 (d, $J$ = 2.5 Hz, 1H), 3.15-3.11 (m, 4H), 3.01-2.99 (m, 4H). $^{13}$C NMR (125 MHz, 298 K, DMSO-$d_6$): δ 163.2, 162.6, 157.0, 133.0, 131.5, 131.3, 129.6, 126.3, 125.6, 122.5, 115.3, 115.0, 80.0, 73.2, 56.5, 54.4, 29.3, 19.04. HR-ESI-MS m/z: $[M+Na]^+$ calcd for $[C_{19}H_{18}N_3O_2]^+$, 320.1382; found, 320.1385.

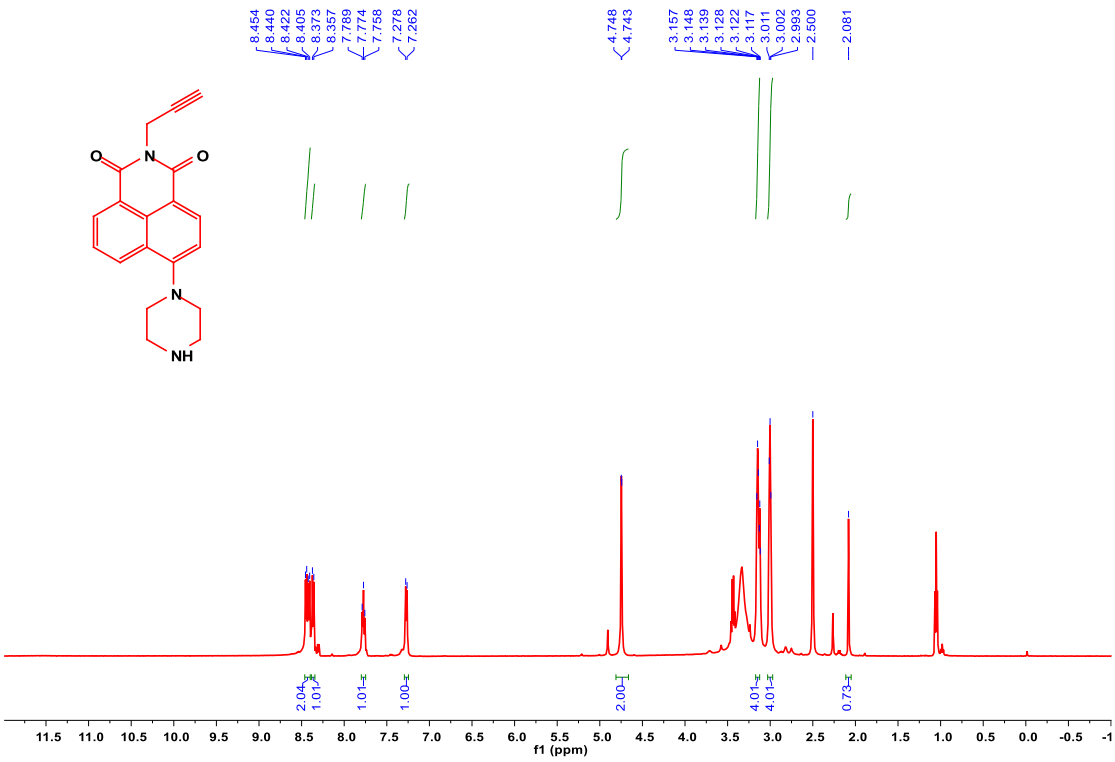


**Fig. S16**. $^{1}$H NMR spectrum of **Compound 2**.

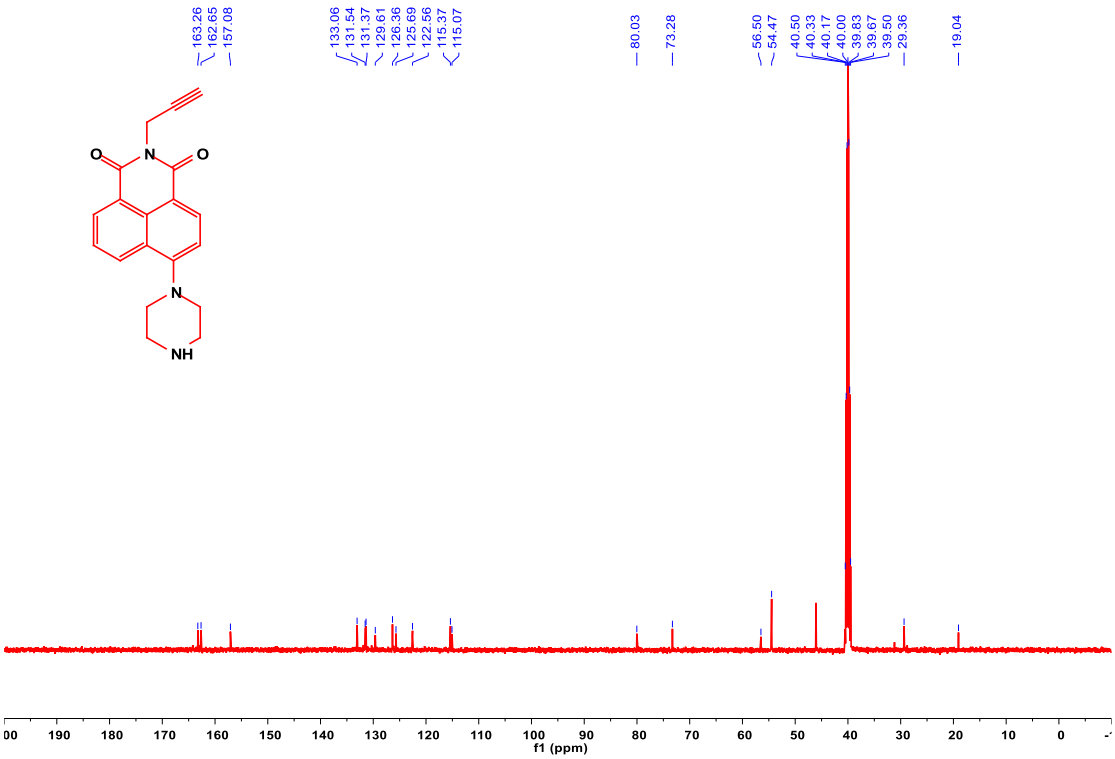


**Fig. S17**. $^{13}$C NMR spectrum of **Compound 2**.

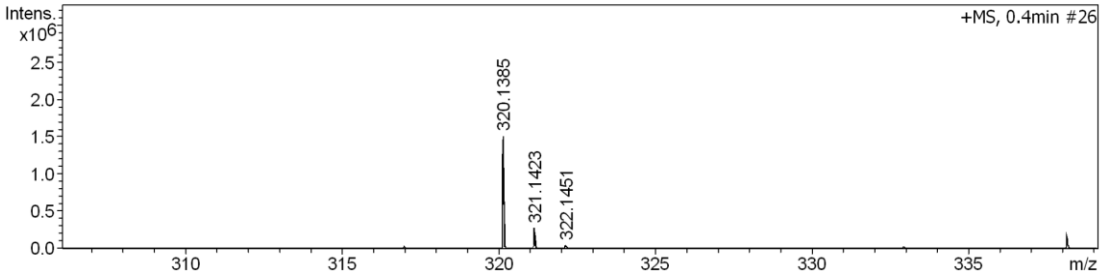


**Fig. S18**. HR-MS spectrum of **Compound 2**.

**Synthesis of Compound 3:** Dissolve the Compound 2 (320 mg, 1 mmol) and 7-hydroxy-2-oxo-2H-chromene-3-carboxylic acid (290 mg, 1.4 mmol) in DCM solution, then HOBT (190 mg, 1.4mmol), EDCI (382 mg, 2mmol) and $NEt_3$ (0.8 ml, 4 mmol) were added in the mixed solution, stirred the mixture over night for 24 h at room temperature. Then, the reaction mixture was concentrated under vacuum, and the crude product was purified by silica column chromatography to obtain **Compound 3.** $^1$H NMR (500 MHz, 298 K, DMSO-$d_6$): δ 10.79 (s, 1H), 8.58-8.56 (d, *J* = 8.5 Hz, 1H), 8.53-8.52 (d, *J* = 7.5 Hz, 1H), 8.18 (s, 1H), 7.87-7.84 (m, 1H), 7.63-7.62 (d, *J* = 9.0 Hz, 1H), 7.40-7.38 (d, *J* = 8.0 Hz, 1H), 6.86-6.84 (m, 1H), 6.78-6.77 (d, *J* = 2.5 Hz, 1H), 4.77 (d, *J* = 2.5 Hz, 1H), 3.71 (s, 2H), 3.31 (s, 2H), 3.30-3.24 (m, 2H), 3.23 (s, 2H), 3.14-3.13 (t, *J* = 7.5 Hz, 1H). $^{13}$C NMR (125 MHz, 298 K, DMSO-$d_6$): δ 164.1, 163.2, 162.6, 158.1, 156.1, 156.0, 143.9, 132.9, 131.5, 131.4, 130.9, 129.5, 126.8, 125.9, 122.6, 120.1, 116.1, 116.0, 114.1,111.2, 102.5, 79.9, 73.3, 53.1, 53.0, 29.4. HR-ESI-MS m/z: $[M+Na]^+$ calcd for $[C_{29}H_{21}N_3O_6Na]^+$, 530.1330; found, 530.1329.

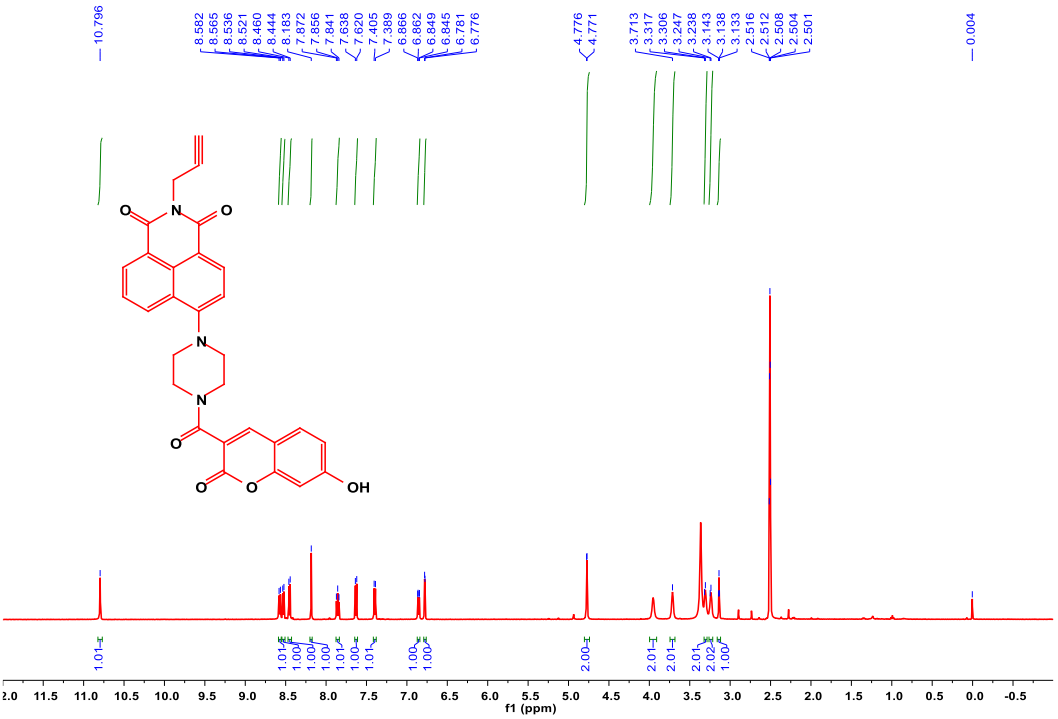


**Fig. S19**. $^{1}$H NMR spectrum of **Compound 3**.

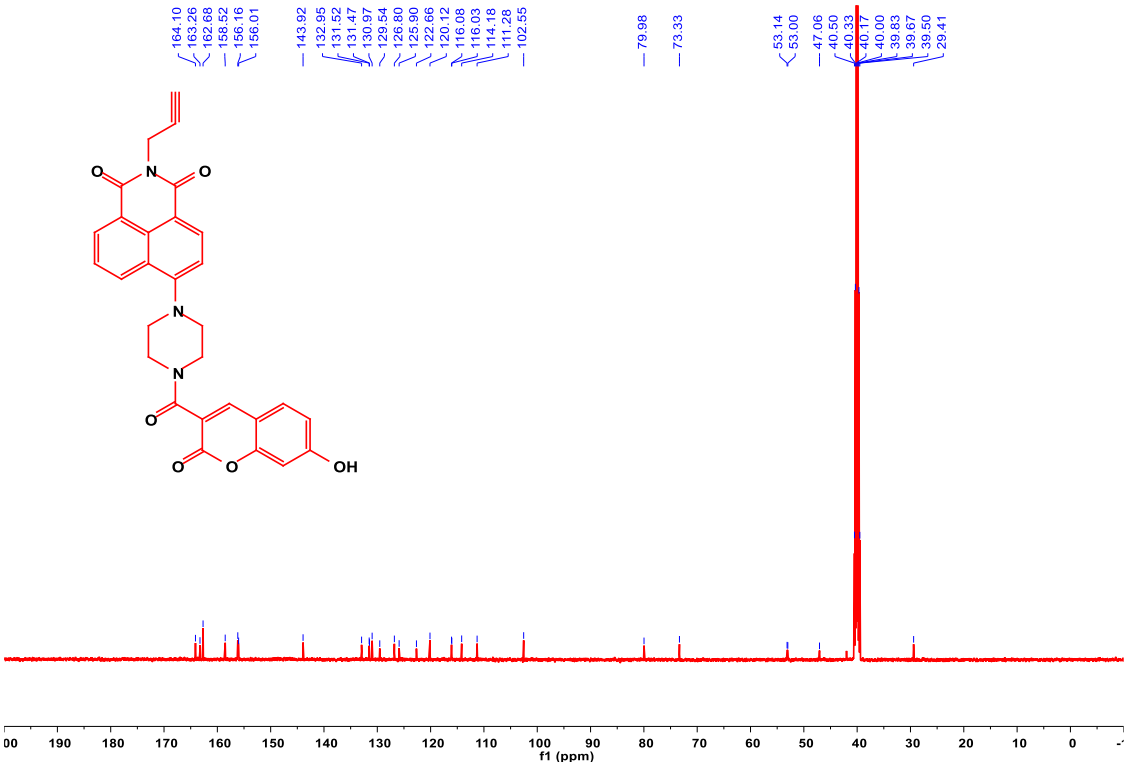


**Fig. S20**. $^{13}$C NMR spectrum of **Compound 3**.

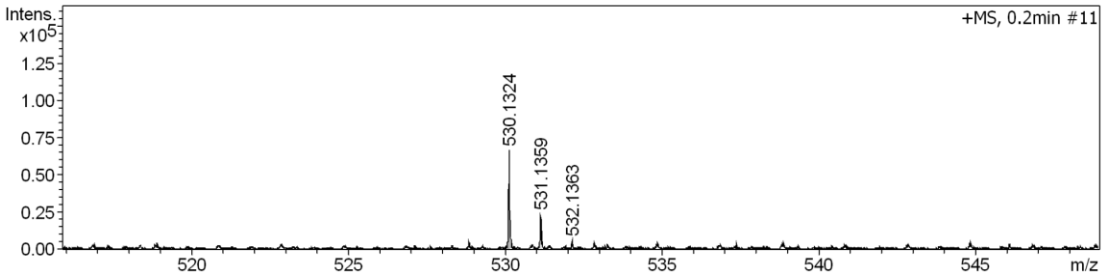


**Fig. S21**. HR-MS spectrum of **Compound 3**.

**Synthesis of Compound 4:** Dissolve the Compound 3 (507 mg, 1 mmol) and MAO-4 (290 mg, 1.4 mmol) in anhydrous DMF of 10 ml. Heat the reactant solution to 100 °C and stir for 12 h under $N_2$ atmosphere. Cool the mixture to room temperature and remove the solvent by reduced pressure distillation. Then, the reaction mixture was concentrated under vacuum, and the crude product was purified by silica column chromatography (PE: EA=4:1, v/v) to obtain **compound 4.** $^1$H NMR (500 MHz, 298 K, $CDCl_3$-*d*): δ 8.65 (d, *J* = 1.0 Hz, 1H), 8.64 (d, *J* =1.0 Hz, 1H), 8.57-8.58 (d, *J* = 8.0 Hz, 1H), 8.00 (s, 1H), 7.84-7.70 (m, 5H), 7.49-7.47 (d, *J* = 8.5 Hz, 1H), 7.40 (d, *J* = 2.0 Hz, 1H), 7.26-6.88 (m, 5H), 5.04 (s, 2H), 4.95 (d, *J* = 2.5 Hz, 1H), 4.13-4.10 (m, 4H), 3.97-3.94 (m, 2H), 3.73 (s, 2H), 3.36-3.32 (m, 4H), 2.27 (m, 2H), 2.18 (s, 1H). $^{13}$C NMR (125 MHz, 298 K, DMSO-$d_6$): δ 168.4, 163.9, 163.2, 162.6, 158.4, 160.0, 155.9, 154.1, 143.5, 134.6, 132.9, 132.2, 131.5, 130.6, 130.1, 129.6, 129.5, 128.7, 126.8. 125.9, 123.3, 122.6, 121.6, 121.3, 116.0, 113.9, 112.5, 101.9, 79.9, 73.3, 69.4, 67.3, 35.5, 29.4, 28.0. HR-ESI-MS m/z: $[M+H]^+$ calcd for $[C_{47}H_{36}ClN_4O_9]^+$, 835.2171; found, 835.2176.

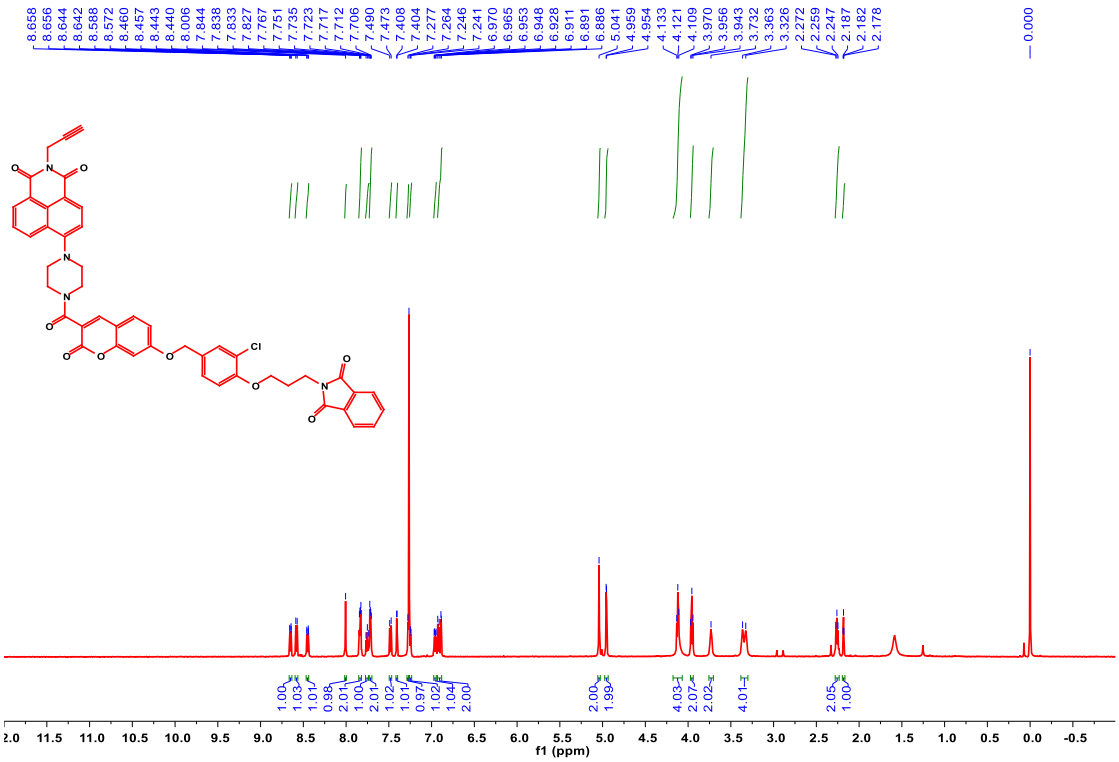


**Fig. S22**. $^{1}$H NMR spectrum of **Compound 4**.

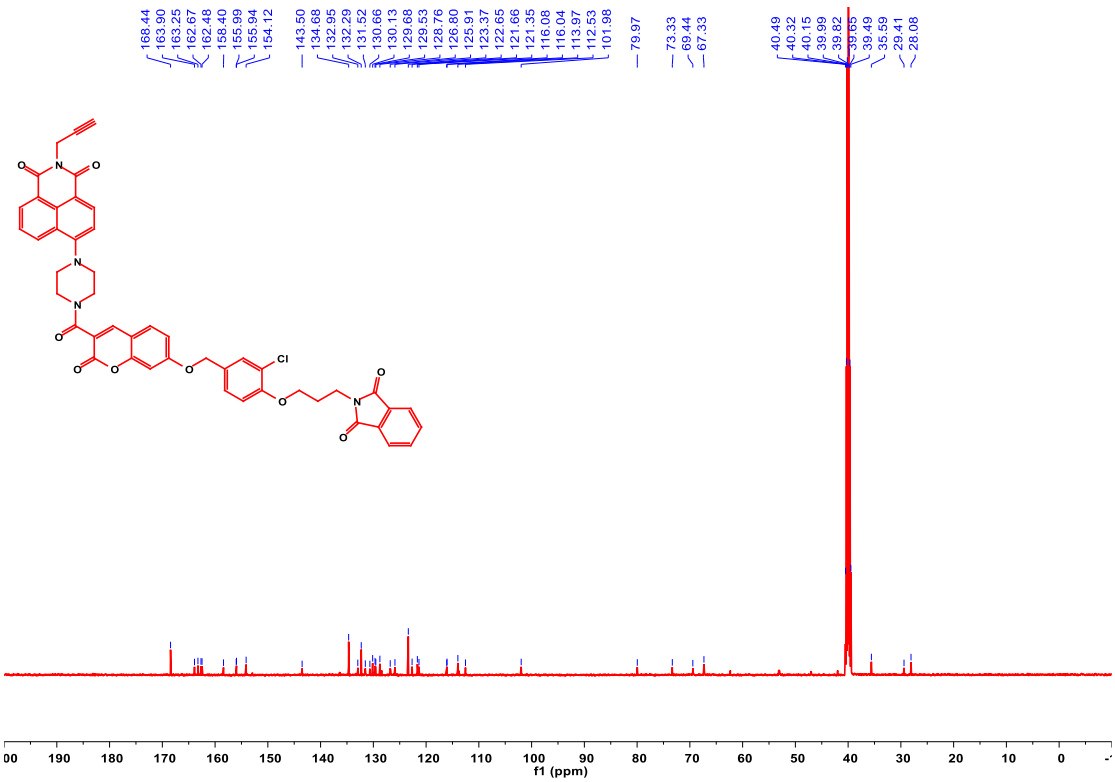


**Fig. S23**. $^{13}$C NMR spectrum of **Compound 4**.

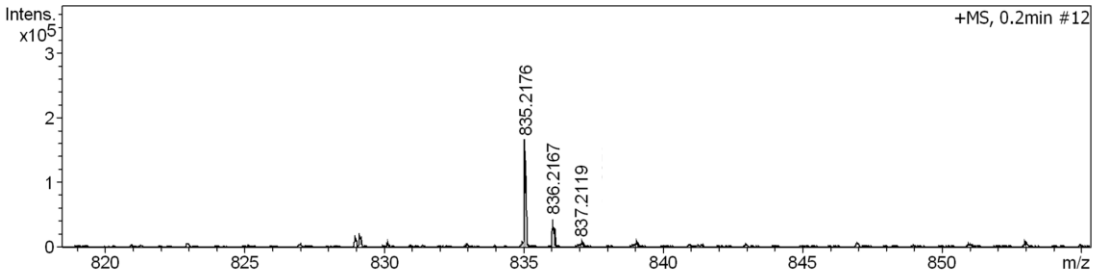


**Fig. S24**. HR-MS spectrum of **Compound 4**.

**Synthesis of Compound 5:** Dissolve the Compound 4 (340 mg, 0.4 mmol), (3-azidopropyl)-triphenylphosphonium hexafluorophosphate (300 mg, 0.6 mmol), Copper sulfate pentahydrate (150 mg, 0.6 mmol) and L-Ascorbic Acid Sodium Salt (240 mg, 1.4 mmol) in anhydrous DMF of 20 ml. Heat the reactant solution to 100 °C and stir for 12 h under $N_2$ atmosphere. Cool the mixture to room temperature and remove the solvent by reduced pressure distillation. Then, the reaction mixture was concentrated under vacuum, and the crude product was purified by silica column chromatography (DCM: MeOH=100:1, v/v) to obtain **Compound 5.** $^1$H NMR (500 MHz, 298 K, DMSO-$d_6$): δ 8.57-8.56 (d, *J* = 8.5 Hz, 1H), 8.50-8.48 (d, *J* = 7.5 Hz, 1H), 8.42-8.41 (d, *J* = 8.0 Hz, 1H), 8.21 (s, 1H), 8.06 (s, 1H), 7.89-7.80 (m, 9H), 7.74-7.71 (m, 12H), 7.50 (d, *J* = 2.0 Hz, 1H), 7.40-7.38 (m, 2H), 7.14-7.09 (m, 3H), 5.29 (s, 2H), 5.16 (s, 2H), 4.46-4.44 (m, 2H), 4.13-4.11 (m, 2H), 3.96 (s, 2H), 3.8-3.79 (d, *J* =6.5 Hz, 2H), 3.78-3.22 (m, 6H), 2.11-2.07 (m, 4H). $^{13}$C NMR (125 MHz, 298 K, DMSO-$d_6$): δ 168.4, 163.8, 163.7, 163.1, 162.4, 158.4, 155.9, 154.1, 135.4, 134.6, 134.0, 133.9, 132.2, 130.7, 130.6, 130.1, 129.6, 128.7, 126.7, 125.8, 124.1, 123.3, 122.9, 121.6, 121.3, 118.8, 116.3, 116.0, 113.9, 112.5, 69.4, 67.3, 56.4, 53.1, 49.5, 47.0, 35.5, 31.1, 28.0, 23.4. HR-ESI-MS m/z: $[M\text{-}PF_6^-]^+$ calcd for $[C_{68}H_{56}ClN_7O_9P]^+$, 1138. 3566; found, 1138. 3568.

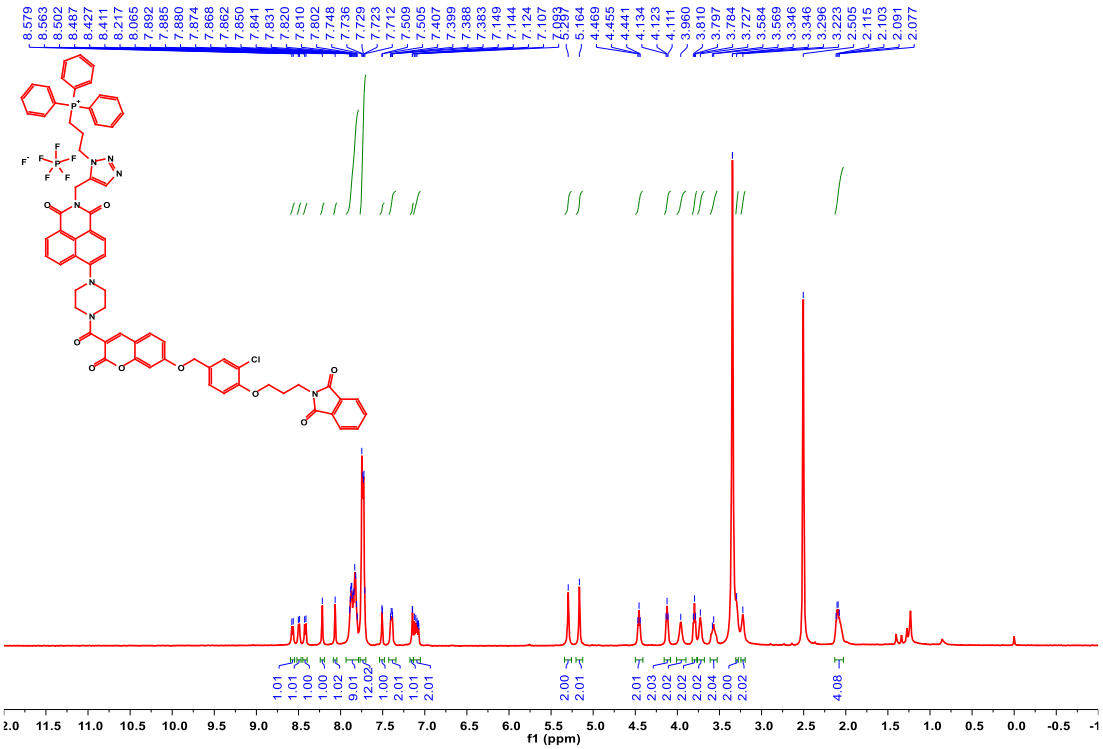


**Fig. S25**. $^{1}$H NMR spectrum of **Compound 5**.

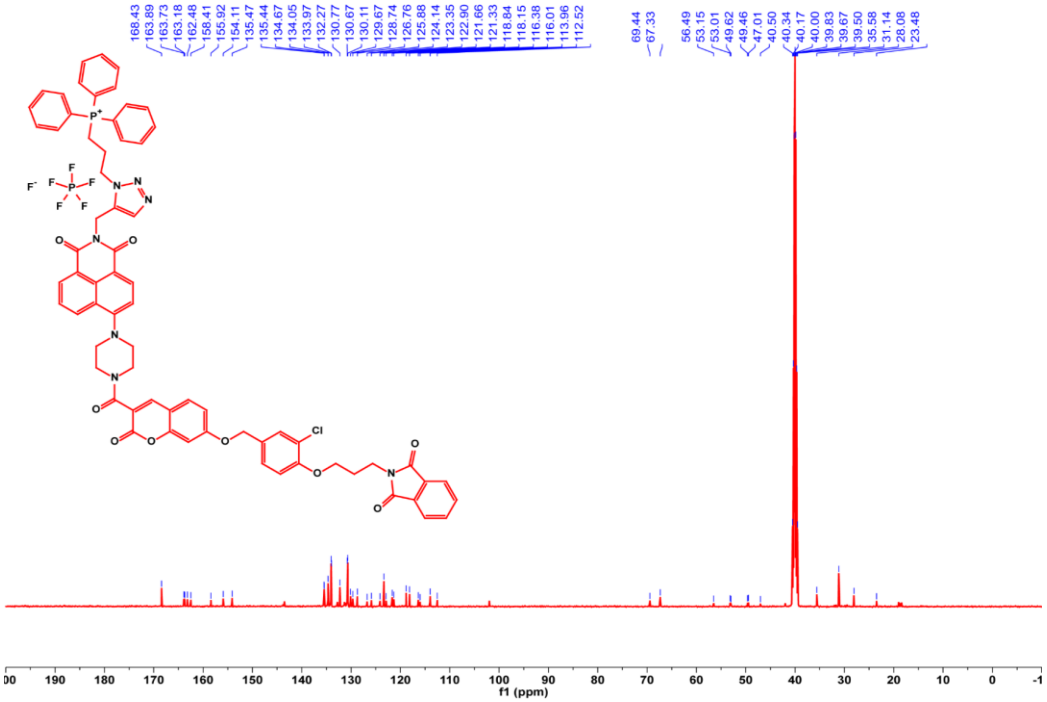


**Fig. S26**. $^{13}$C NMR spectrum of **Compound 5**.

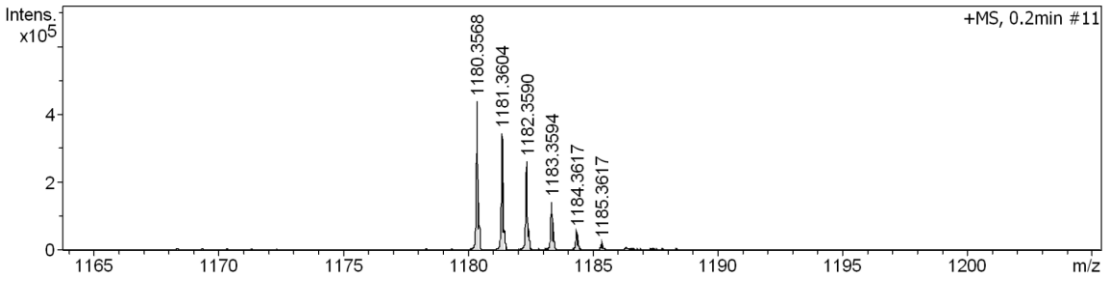


**Fig. S27**. HR-MS spectrum of **Compound 5**.

**Synthesis of Compound TMF2P:** Dissolve the Compound 5 (265 mg, 0.2 mmol) was dissolved in THF (10 mL). Heat the solution to 50 ºC. And hydrazine monohydrate (65%, 0.4 mL, 5 mmol) was added into the solution. Then the reaction mixture was stirred at 50ºC for 5h under argon atmosphere. Subsequently, saturated aqueous $Na_2CO_3$ (10 mL) was poured into the mixture. Extracted with $CH_2Cl_2$ (2 × 20 mL). Dry the organic layer and combine over anhydrous $Na_2SO_4$ and concentrate under reduced pressure to obtain compound **TMF2P** as bright yellow solid through a silica gel column using DCM-MeOH (100:1, v/v). $^1$H NMR (500 MHz, 298 K, DMSO-$d_6$): 8.58-8.57 (d, $J$ =7.0 Hz, 1H), 8.51-8.50 (d, $J$ =6.0 Hz, 1H), 8.43-8.42 (d, $J$ =6.5 Hz, 1H), 8.17 (s, 1H), 8.06 (s, 1H), 7.88-7.72 (m, 18H), 7.63-7.62 (d, $J$ =6.5 Hz, 1H), 7.40-7.39 (d, $J$ =7.0 Hz, 1H), 6.86-6.84 (d, $J$ =7.0 Hz, 2H), 6.77 (s, 1H), 5.03 (s, 2H), 4.95-4.94 (d, $J$ =2.5 Hz, 2H), 4.12-4.10 (m, 4H), 3.86-3.93 (m, 2H), 3.72 (s, 2H), 3.53 (m, 4H), 2.26-2.16 (m, 3H). $^{13}$C NMR (125 MHz, 298 K, DMSO-$d_6$): δ 167.0, 162.9, 162.48, 158.2, 155.6, 153.8, 135.4, 135.4, 134.6, 134.0, 133.9, 132.2, 130.7, 130.6, 130.1, 127.7, 125.7, 124.8, 123.14, 122.2, 121.7, 120.3, 120.3, 117.5, 117.2, 115.2, 115.0, 112.0, 69.0, 66.92, 56.0, 52.3, 52.1, 48.8, 48.7, 46.9, 35.4, 30.9, 27.4, 23.1. HR-ESI-MS m/z: $[M\text{-}PF_6^-]^+$ calcd for $[C_{60}H_{54}ClN_7O_7P]^+$, 1051. 3580; found, 1051. 3586.

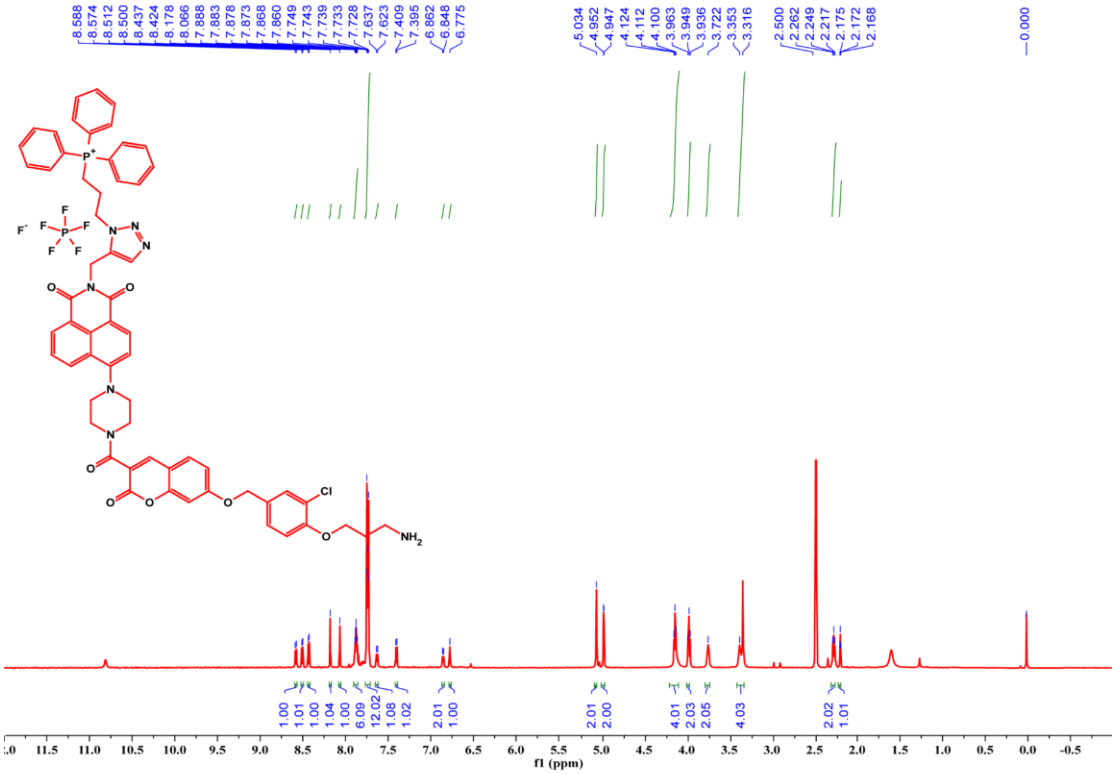

**Fig. S28**. $^{1}$H NMR spectrum of **TMF2P**.

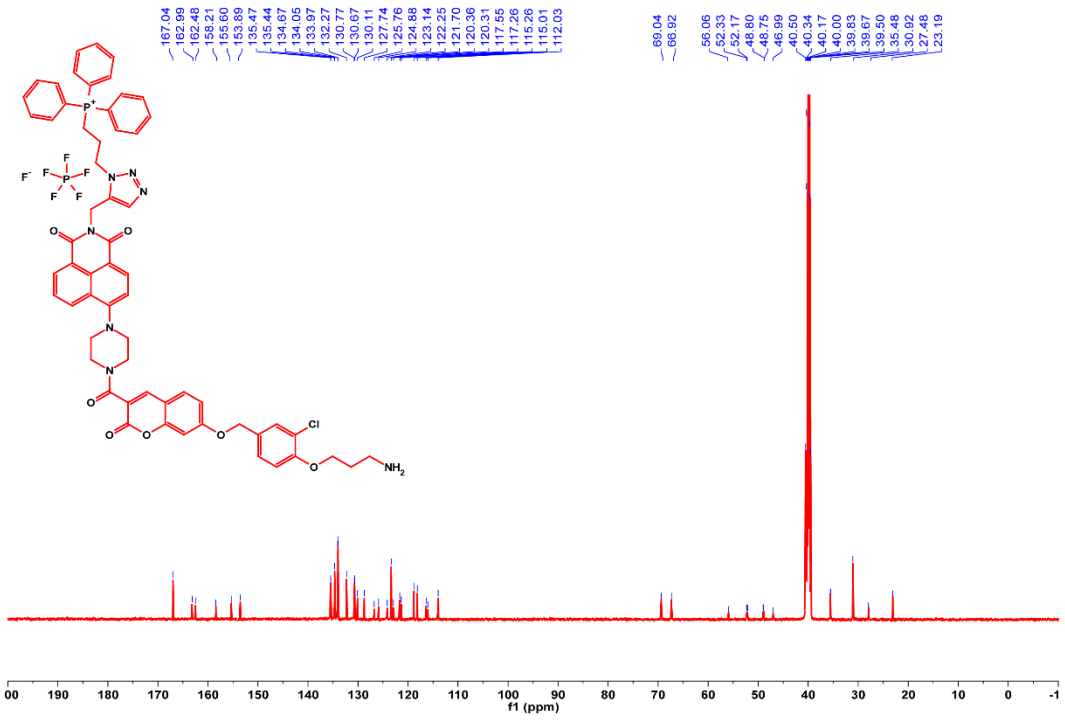

**Fig. S29**. $^{13}$C NMR spectrum of **TMF2P**.

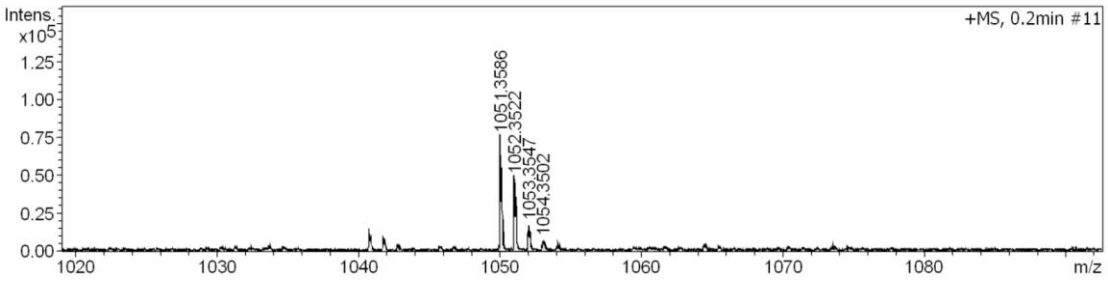


**Fig. S30**. HR-MS spectrum of **TMF2P**.

## 3. Basic spectral properties of TMF2P.

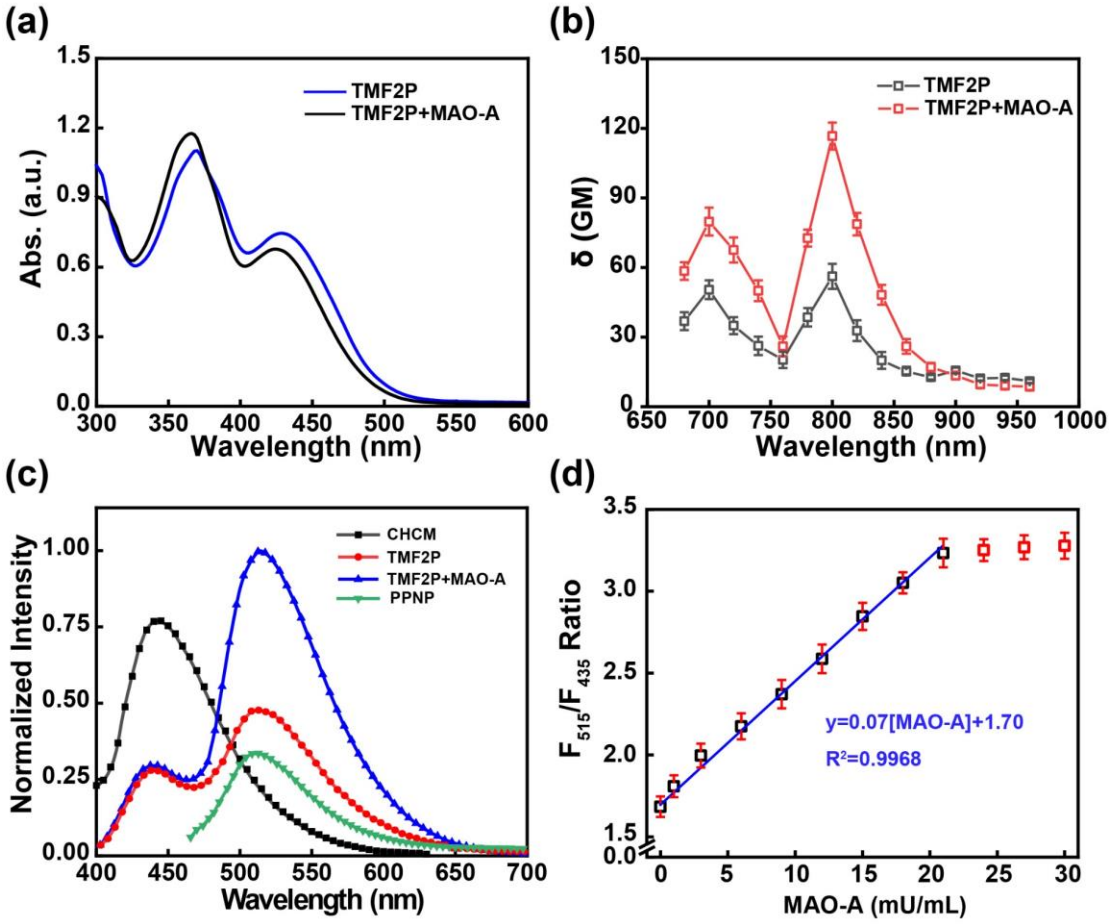


**Fig. S31**. (a) UV-vis absorption spectra of **TMF2P** probe before (blue line) and after (black line) addition of MAO-A. (b) Two-photon fluorescence spectra of **TMF2P** probe before (black line) and after (red line) addition of MAO-A. (c) (c) Two-photon fluorescence spectra of CHCM, PPNP, **TMF2P**, and **TMF2P** reacted with MAO-A ($\lambda_{ex}$ = 700 nm). (e) The plot of $F_{515}$ / $F_{435}$ ratios ($F_{515}$: 490 – 550 nm, $F_{435}$: 400 – 475 nm) of the **TMF2P** probe versus the MAO-A concentrations (1 - 30 mU $mL^{-1}$). error bars, n = 10, S.D.

## 4. Stabilities of TMF2P probe toward detection of MAO-A

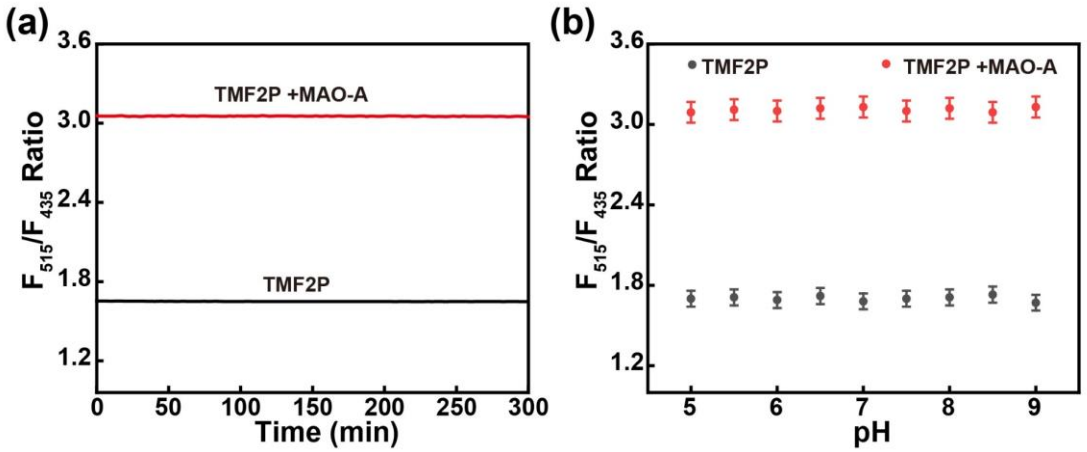


**Fig. S32**. (a) Time stabilities of **TMF2P** probe (5 μM) with (red curve) and without (black curve) MAO-A (20 mU $mL^{-1}$). (b) pH stabilities of **TMF2P** probe (5 μM) with (red curve) and without (black curve) MAO-A (20 mU $mL^{-1}$). error bars, n = 10, S.D.

## 5. Competition tests of TMF2P probe toward determination of MAO-A

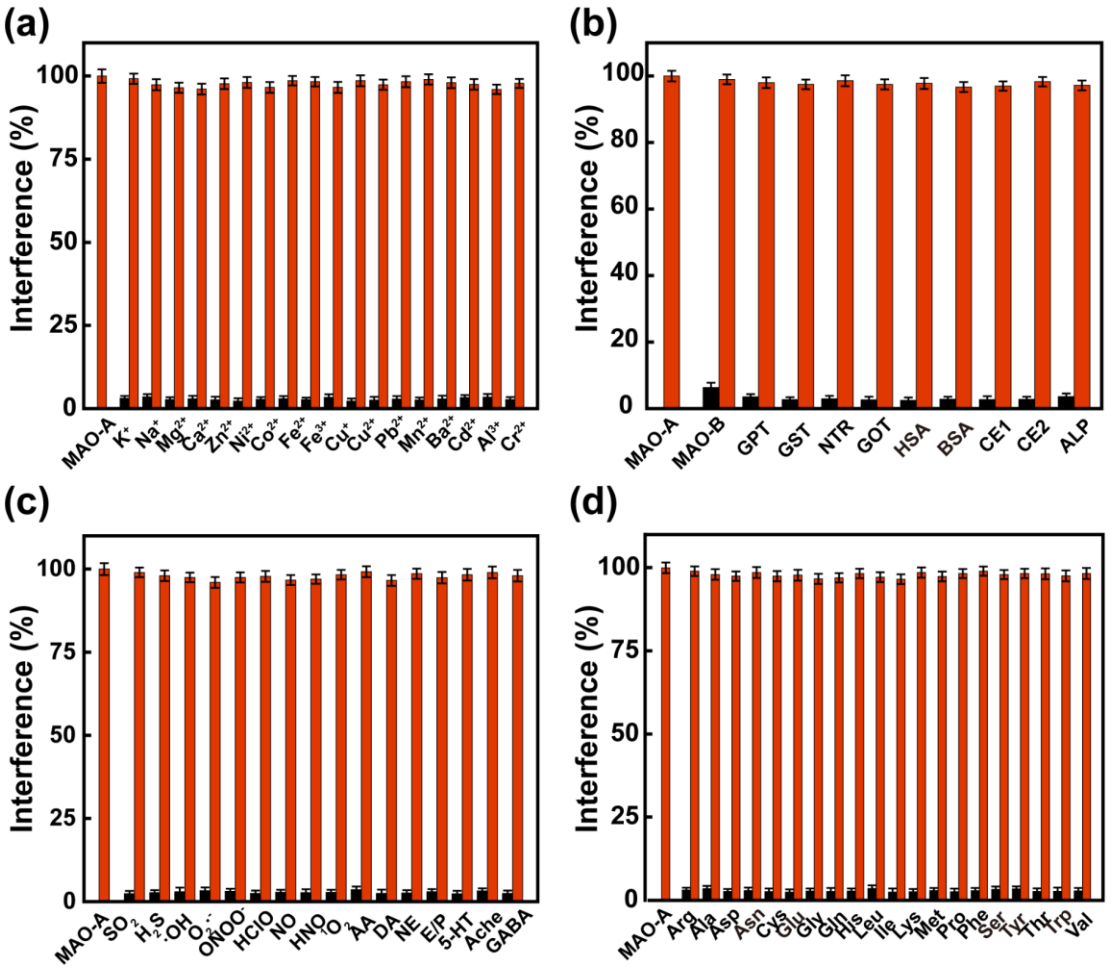


**Fig. S33**. Competition tests of 5.0 μM **TMF2P** probe toward MAO-A followed by addition of (a) metal ions (1.0 mM for each) (b) proteins (100 mU for each). (c) ROS and other relative analyts (1.0 mM for each). (d) amino acids (1.0 mM for each) (error bars, n = 10, S.D.).

## 6. Sensing mechanism of TMF2P probe

The mechanism studies were carried out to further understand the molecular interactions between **TMF2P** and MAO-A. Firstly, high resolution mass spectroscopy (HR-MS) was used to investigate the reaction of **TMF2P** with MAO-A, in which a mass to charge value (m/z) of 853.2883 belonging to [**TMP**-$PF_6^-$]$^+$ and 57.0260 belonging to acrylaldehyde were found (Fig. S34a-b), indicating that the chloro-substituted phenyl-propylamine (PA) moiety was cleaved from the probe and the product **TMP** was formed. The reaction mechanism of the **TMF2P** to MAO-A was based on oxidative deamination, followed by β-elimination and finally the PA part was cleaved from **TMF2P** (Fig. S34c).

**(a)**

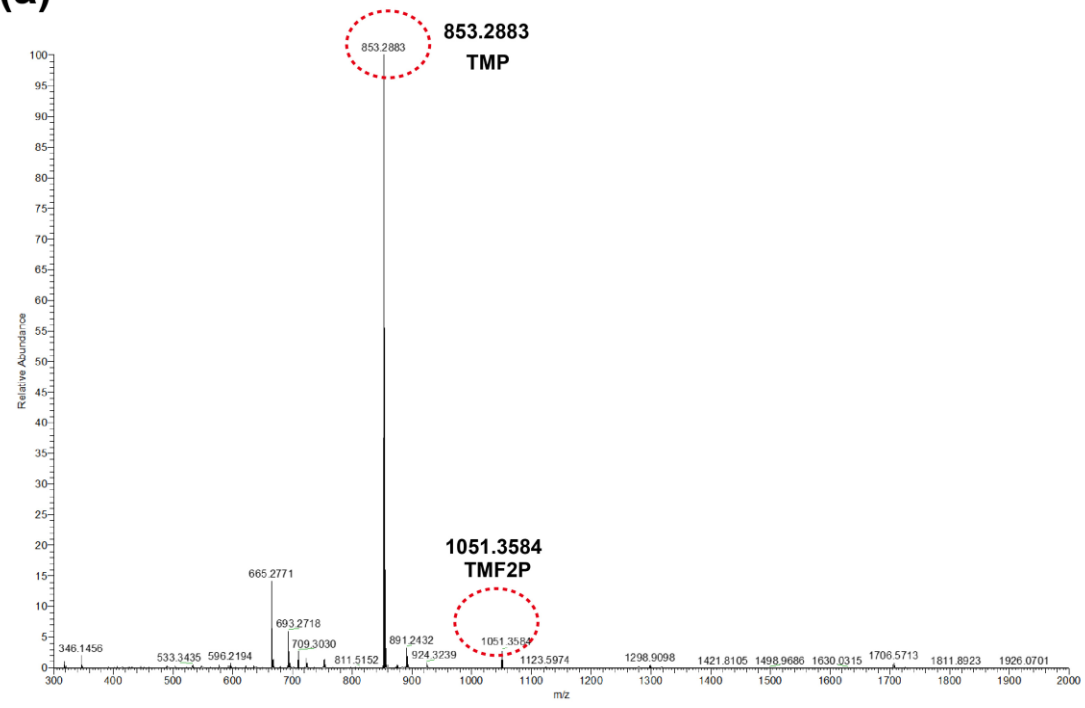

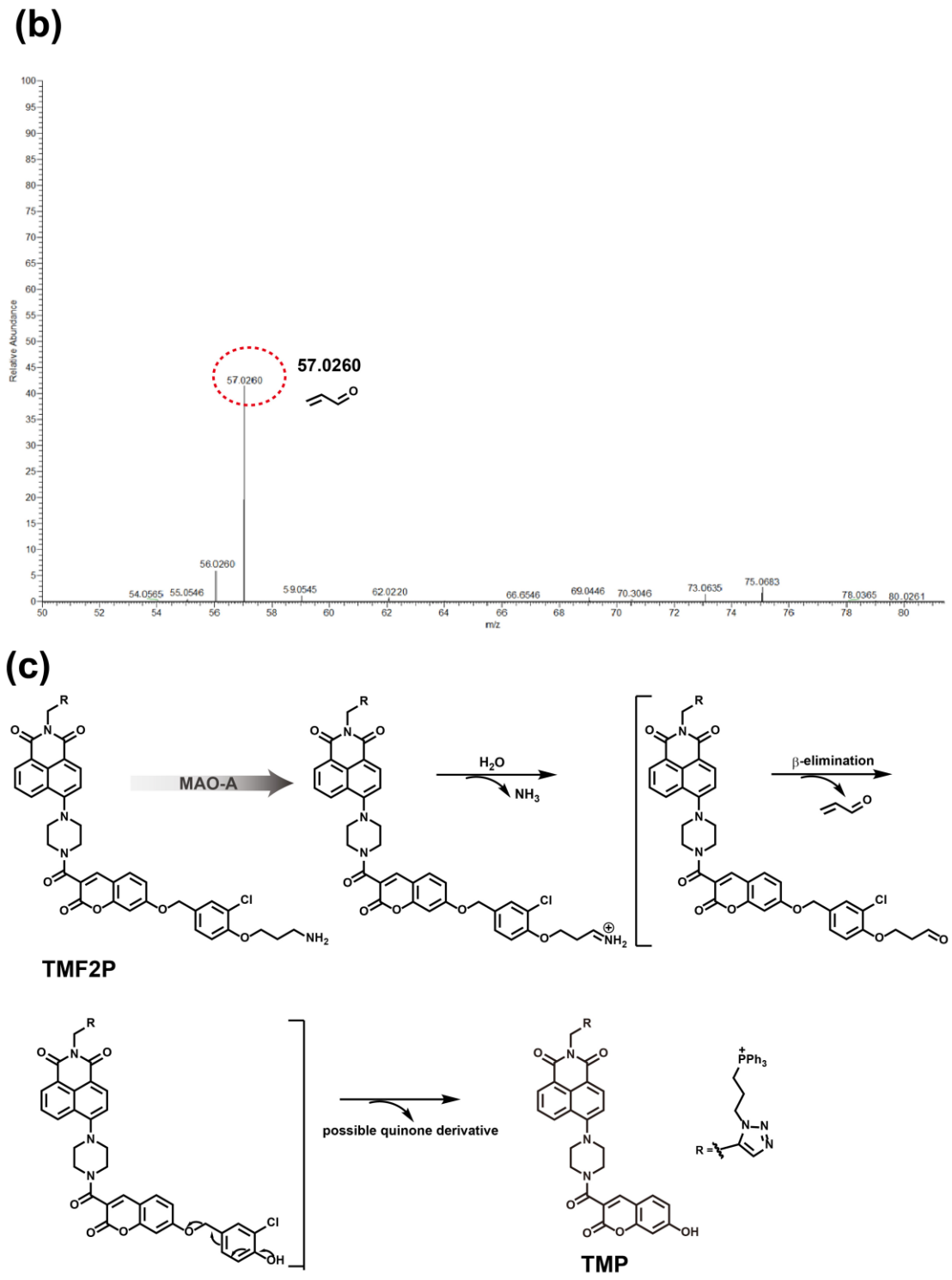


**Fig. S34.** (a) HR-MS of **TMF2P** probe after interacted with MAO-A to **TMP**. (b) HR-MS of **TMF2P** probe after interacted with MAO-A to form acrylaldehyde. (c) Proposed reaction mechanism of the **TMF2P** to MAO-A.

## 7. The density functional theory (DFT) analysis.

All calculations were performed with Density Functional Theory (DFT) using the Gaussian16 program.[S5] The molecular structures were optimized using the B3LYP functional and 6-31G(d) basis set with the DFT-D3 correction and the Solvation Density Model (SMD).[S6-8] The highest occupied molecular orbital (HOMO), the lowest unoccupied molecular orbital (LUMO) and the orbitals of HOMO-1 and LUMO-1 were obtained at the same level.

The density functional theory (DFT) calculations were also performed to study the ICT process in **TMF2P**. The HOMO-1 of **TMF2P** was mainly distributed on the PA moiety, while that of **TMP** was mainly on the CM moiety; the LUMO+1 of **TMF2P** and **TMP** were mainly distributed on the CM moiety. Thus, the ICT process between hydroxyl group and CM in **TMP** can be supported by the results of DFT calculations (Fig. S35).

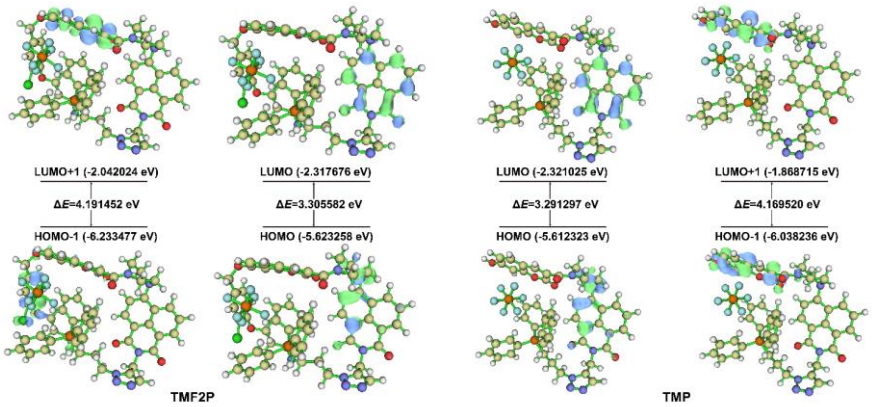


**Fig. S35.** HOMO−LUMO energy levels of **TMF2P** and **TMF2P**+MAO-A.

## 8. FACS and MTT measurements of TMF2P probe in live cells

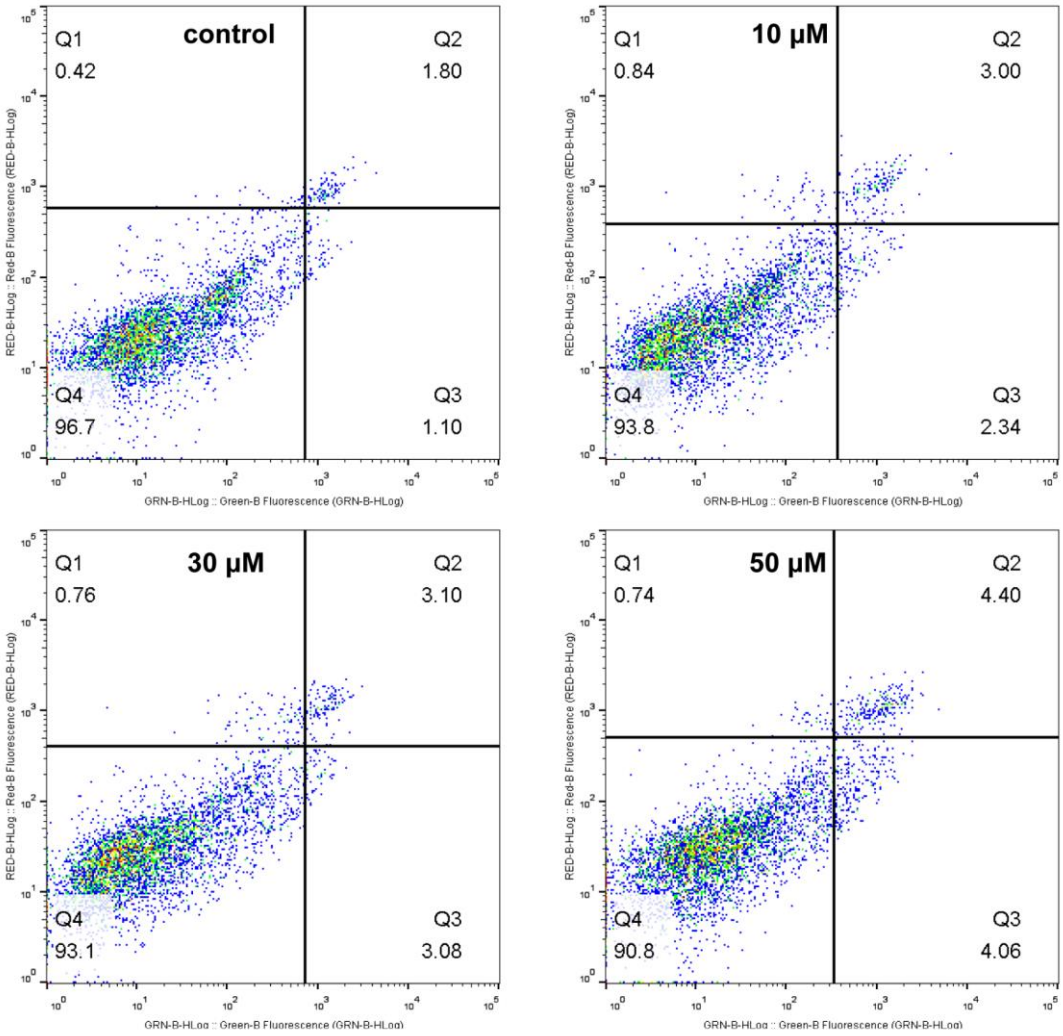


**Fig. S36.** The apoptosis assay of neurons incubated with **TMF2P** probe under different concentrations (a) 0 μM, (b) 10 μM, (c) 30 μM, and (d) 50 μM for 24 h. Q1, Q2, Q3, and Q4 represent the regions of dead neurons, late apoptotic neurons, early apoptotic neurons, and normal neurons, respectively.

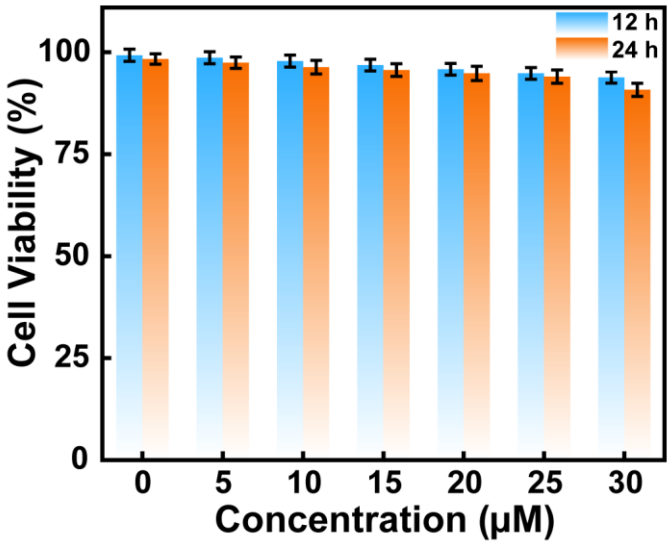


**Fig. S37**. The MTT assay for neurons upon incubation with **TMF2P** at different concentrations (0, 5, 10, 15, 20, 25 and 30 μM) after 12 h and 24 h, respectively (error bars, n = 10, S.D.).

## 9. Two-photon microscope imaging and quantification of mitochondrial MAO-A in response to $O_2^{\bullet-}$ stimulation.

The acquisition and cultivation of neurons were conducted as a previous reported procedure.[S4] Newborn within 24 h C57BL/6 wild-type mice were anesthetized by halothane, and then their brains were removed quickly and put in Hanks' balanced salt solution (HBSS, free of $Mg^{2+}$ and $Ca^{2+}$) at 0 °C. Tissues of the cortex were stripped out and then incubated with papain at 37 °C for 12 min, after that the they were dispersed into poly-d-lysine-coated 35 mm Petri dishes at a density of 1 $\times 10^6$ cells/dish. The neurons were cultured with neurobasal medium containing L-Glutamine and B27 and the medium was changed three times a week. After maintained at 37 °C in a humidified atmosphere with 5% $CO_2$ incubator for a week, the neurons could be used for imaging.

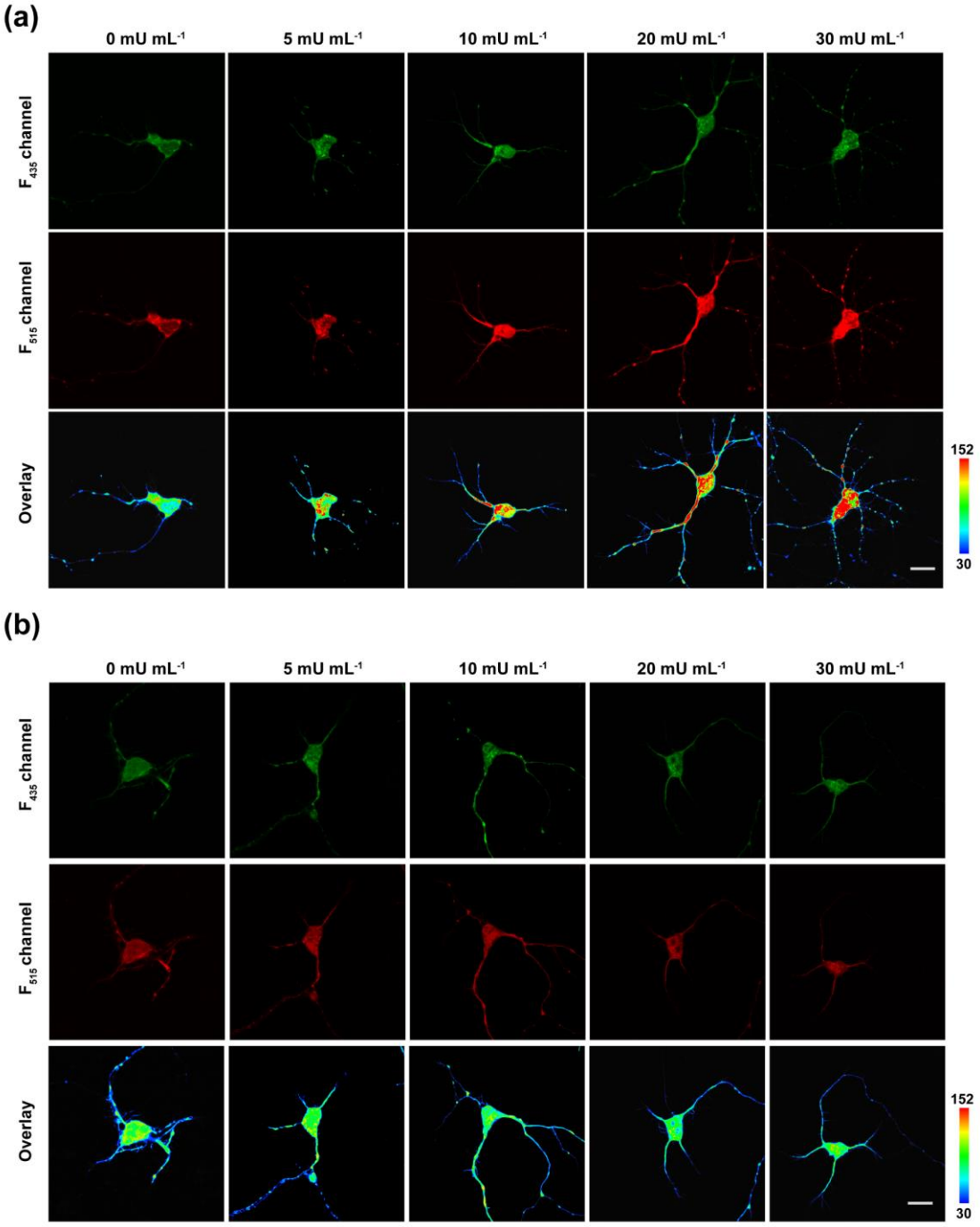


**Fig. S38**. (a) Fluorescence images of **TMF2P** in neurons with the addition of MAO-A with different concentrations (5, 10, 20 and 30 mU $mL^{-1}$). (b) Fluorescence images of neurons with the addition of MAO-B with different concentrations (5, 10, 20 and 30 mU $mL^{-1}$). Scale bar: 15 μm.

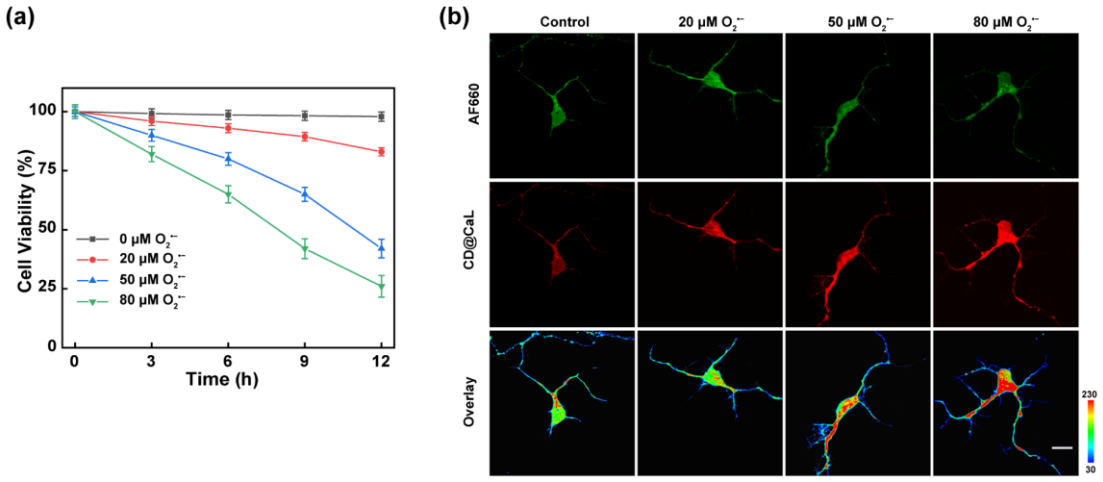


**Fig. S39**. (a) Summarized data of neuron viability stimulated by various concentrations of $O_2^{\bullet-}$ (0, 20, 50, and 80 μM) stimulation for different times (Error bars, n=10, S.D.). (b) Fluorescence images from the $Ca^{2+}$ probe (tDNA-TPP plus CD@CaL plus AF660) of neurons under various concentrations of $O_2^{\bullet-}$ (0, 20, 50, and 80 μM) stimulation. Scale bar: 15 μm.

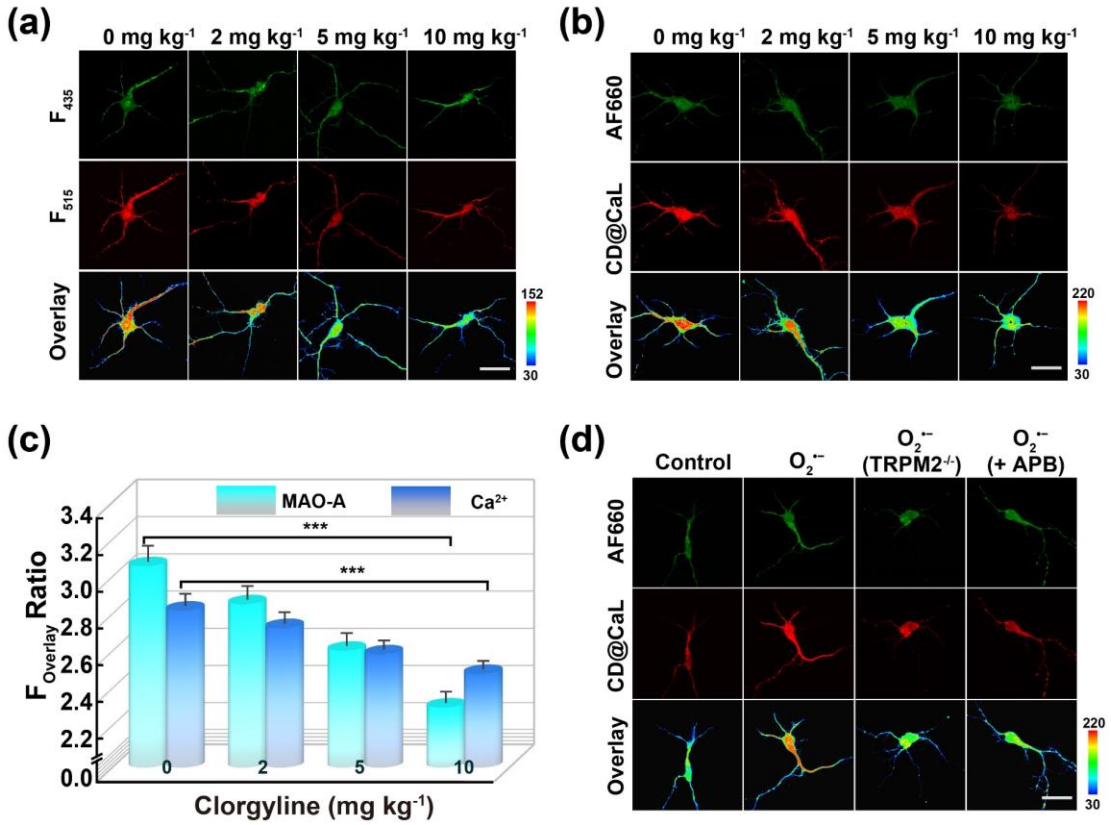


**Fig. S40.** (a) Fluorescence images of neurons incubation of **TMF2P** probe (5 μM) under stimulated 80 μM $O_2^{\bullet-}$, and in the presence of different concentrations Clorgyline (0, 2, 5, 10 mg $kg^{-1}$). (b) Fluorescence images of neurons incubation of $Ca^{2+}$ probe (5 μM) under stimulated 80 μM $O_2^{\bullet-}$, and in the presence of different concentrations Clorgyline (0, 2, 5, 10 mg $kg^{-1}$). (c) Summarized data of MAO-A and $Ca^{2+}$ changes under stimulated 80 μM $O_2^{\bullet-}$, and in the presence of different concentrations Clorgyline (Error bars, n=10, S. D). (d) Fluorescence images of $Ca^{2+}$ in neurons after neurons stimulated by 80 μM $O_2^{\bullet-}$, 80 μM $O_2^{\bullet-}$ in the presence of 100 nM APB and $TRPM2^{-/-}$ neurons stimulated by 80 μM $O_2^{\bullet-}$, respectively. Scale bar: 25 μm. Assume that the significance level of the statistical test is 0.001 (***) (n = 20; ***, $p < 0.001$).

To further verify that MAO-A regulated $Ca^{2+}$ influx in mitochondria via TRPM2 channels, we performed two experiments, the first was stimulating neurons with 0, 10 and 30 mU $mL^{-1}$ of exogenous MAO-A, respectively. We clearly observed dose-dependent relationship between $Ca^{2+}$ level and MAO-A levels. And the level of $Ca^{2+}$ in TRPM2$^{-/-}$ neurons was significantly lower than that of WT neurons as shown in Fig. 4c and Fig. S41. The second experiment was stimulating WT neurons in the presence of 100 nM Aminoethyl diphenylborinate (APB, a known inhibitor of TRPM2 channel) with exogenous MAO-A, the results were consistent with those obtained from TRPM2$^{-/-}$ neurons.

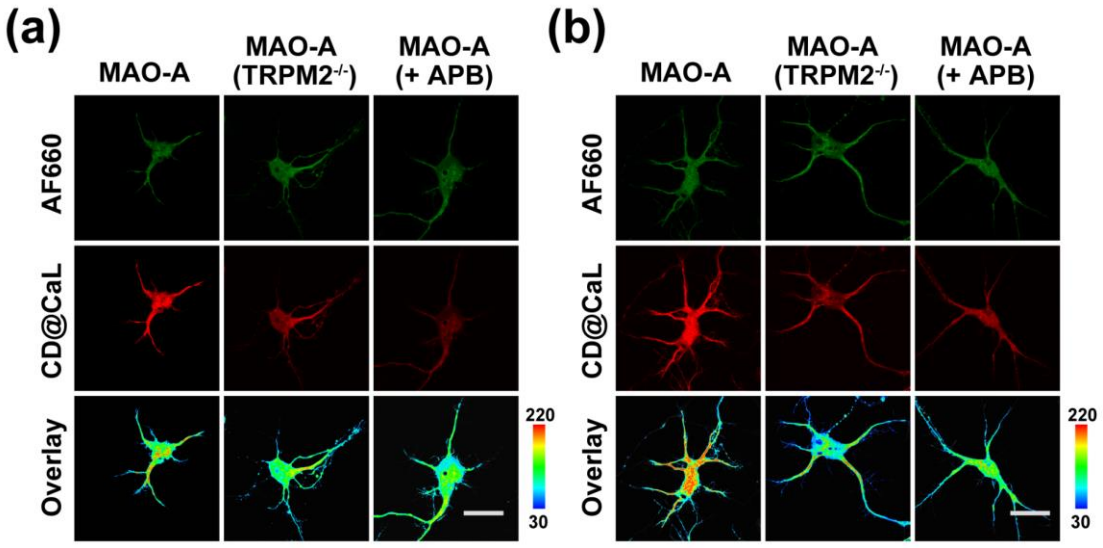


**Fig. S41.** (a) Fluorescence images of $Ca^{2+}$ in neurons after stimulated by 10 mU $mL^{-1}$ MAO-A, 10 mU $mL^{-1}$ MAO-A in the presence of 100 nM APB and TRPM2$^{-/-}$ neurons stimulated by 10 mU $Ml^{-1}$ MAO-A, respectively. (b) Fluorescence images of $Ca^{2+}$ in neurons after neurons stimulated by 30 mU $mL^{-1}$ MAO-A, 30 mU $mL^{-1}$ MAO-A in the presence of 100 nM APB and TRPM2$^{-/-}$ neurons stimulated by 30 mU $mL^{-1}$ MAO-A, respectively. Scale bar: 15 μm.

## 10. References

S1. Fridovich, I. Quantitative Aspects of the Production of Superoxide Anion Radical by Milk Xanthine Oxidase. *J. Biol. Chem.* **1970**, *245*, 4053-4057.

S2. Xu, K. H.; Liu, X.; Tang, B.; Yang, G. W.; Yang, Y.; An, L. G. Design of a Phosphinate-Based Fluorescent Probe for Superoxide Detection in Mouse Peritoneal Macrophages. *Chem-Eur. J.* **2007**, *13*, 1411-1416.

S3. Wu, X. F.; Shi, W.; Li, X. H.; Ma, H. M. A Strategy for Specific Fluorescence Imaging of Monoamine Oxidase A in Living Cells. *Angew. Chem. Int. Ed.* **2017**, *56*, 15319–5323.

S4. Liu, Z. C.; Pei, H.; Zhang, L. M.; Tian, Y. Mitochondria-Targeted DNA Nanoprobe for Real Time Imaging and Simultaneous Quantification of $Ca^{2+}$ and pH in Neurons. *ACS Nano.* **2018**, *12*, 12357-12368.

S5. Frisch, M. J.; Trucks, G. W.; Schlegel, H. B.; Scuseria, G. E.; Robb, M. A.; Cheeseman, J. R.; Scalmani, G.; Barone, V.; Mennucci, B.; Petersson, G. A.; Nakatsuji, H.; Caricato, M.; Li, X.; Hratchian, H. P.; Izmaylov, A. F.; Bloino, J.; Zheng, G.; Sonnenberg, J. L.; Hada, M.; Ehara, M.; Toyota, K.; Fukuda, R.; Hasegawa, J.; Ishida, M.; Nakajima, T.; Honda, Y.; Kitao, O.; Nakai, H.; Vreven, T.; Montgomery Jr., J. A.; Peralta, J. E.; Ogliaro, F.; Bearpark, M. J.; Heyd, J.; Brothers, E. N.; Kudin, K. N.; Staroverov, V. N.; Kobayashi, R.; Normand, J.; Raghavachari, K.; Rendell, A. P.; Burant, J. C.; Iyengar, S. S.; Tomasi, J.; Cossi, M.; Rega, N.; Millam, N. J.; Klene, M.; Knox, J. E.; Cross, J. B.; Bakken, V.; Adamo, C.; Jaramillo, J.; Gomperts, R.; Stratmann, R. E.; Yazyev, O.; Austin, A. J.; Cammi, R.; Pomelli, C.; Ochterski, J. W.; Martin, R. L.; Morokuma, K.; Zakrzewski, V. G.; Voth, G. A.; Salvador, P.; Dannenberg, J. J.; Dapprich, S.; Daniels, A. D.; Farkas, Ö.; Foresman, J. B.; Ortiz, J. V.; Cioslowski, J.; Fox, D. *J.: Gaussian 16, Revision A.03. Gaussian, Inc.: Wallingford,* CT, USA, **2016**.

S6. Becke, A. D. Density-functional thermochemistry. III. The role of exact exchange. *J. Chem. Phys.* **1993**, *98*, 5648-5652.

S7. Grimme, S; Antony, J; Ehrlich, S; Krieg, H. A consistent and accurate ab initio parametrization of density functional dispersion correction (DFT-D) for the 94 elements H-Pu. *J. Chem. Phys*. **2010** ,*132*, 154104.

S8. Marenich, A. V.; Cramer, C. J.; Truhlar, D. G. Universal solvation model based on solute electron density and on a continuum model of the solvent defined by the bulk dielectric constant and atomic surface tensions. *J. Phys. Chem. B* **2009**, *113*, 6378-6396.